USGS
science for a changing world

Prepared in cooperation with the U.S. Environmental Protection Agency

Coagulant and Sorbent Efficacy in Removing Mercury from Surface Waters in the Cache Creek Watershed, California

Open-File Report 2019–1001

U.S. Department of the Interior
U.S. Geological Survey

Coagulant and Sorbent Efficacy in Removing Mercury from Surface Waters in the Cache Creek Watershed, California

By Erica R. De Parsia, Jacob A. Fleck, David P. Krabbenhoft, Kim Hoang, David Roth, and Paul Randall

Prepared in cooperation with the U.S. Environmental Protection Agency

Open-File Report 2019–1001

U.S. Department of the Interior
U.S. Geological Survey

U.S. Department of the Interior
DAVID BERNHARDT, Acting Secretary

U.S. Geological Survey
James F. Reilly II, Director

U.S. Geological Survey, Reston, Virginia: 2019

Suggested citation:
De Parsia, E.R., Fleck, J.A., Krabbenhoft, D.P., Hoang, K., Roth, D., and Randall, P., 2019, Coagulant and sorbent efficacy in removing mercury from surface waters in the Cache Creek watershed, California: U.S. Geological Survey Open-File Report 2019–1001, 46 p., https://doi.org/10.3133/ofr20191001.

ISSN 2331-1258 (online)

Acknowledgments

We thank our colleagues at the U.S. Environmental Protection Agency, Region IX, especially Wilson Yee, John Hillenbrand, Matthew Small, Joseph Eidelberg, Eugenia McNaughton, and Larry Bradfish for their assistance in the development of project scope, site selection, and logistical support. We are grateful to Todd Muelhoefer at Kinder Morgan, Inc., and J.R. Flanders at EHS Support, LLC, for the Harley Gulch area site information, guidance, and access. We thank our colleagues at the U.S. Geological Survey, California Water Science Center (USGS), especially Angela Hansen, Joan Lopez, and Nicholas Graham for assistance in field and laboratory activities and Charlie Alpers, Peter Bennett, Tamara Kraus, and Liz Stumpner for constructive insights and valuable information contributing to the successful execution of the project. We thank Shane Kiley, Phil Bachand, and Mathew Tinker for valuable information about materials and operations for coagulation and sorbent techniques. We also extend our appreciation to John DeWild at the USGS Wisconsin Mercury Research Laboratory for assistance with laboratory analyses and data quality.

Contents

Figures

Tables

Conversion Factors

International System of Units to U.S. customary units

Multiply	By	To obtain
	Length	
centimeter (cm)	0.3937	inch (in.)
millimeter (mm)	0.03937	inch (in.)
meter (m)	3.281	foot (ft)
kilometer (km)	0.6214	mile (mi)
kilometer (km)	0.5400	mile, nautical (nmi)
meter (m)	1.094	yard (yd)
nanometer (nm)	3.937e-8	inch (in.)
micrometer (µm)	3.937e-5	inch (in.)
	Volume	
cubic meter (m3)	6.290	barrel (petroleum, 1 barrel = 42 gal)
liter per minute (L/min)	1.05669	quart per minute (qt/min)
liter (L)	33.81402	ounce, fluid (fl. oz)
liter (L)	2.113	pint (pt)
liter (L)	1.057	quart (qt)
liter (L)	0.2642	gallon (gal)
milliliter (mL)	0.033814	ounce, fluid (fl. oz)
milliliter (mL)	0.00211338	pint (pt)
milliliter (mL)	0.00105669	quart (qt)
milliliter (mL)	0.000264172	gallon (gal)
microliter (µL)	3.3814e-5	ounce, fluid (fl. oz)
microliter (µL)	2.11338e-6	pint (pt)
microliter (µL)	1.05669e-6	quart (qt)
microliter (µL)	2.64172e-7	gallon (gal)
cubic meter (m3)	264.2	gallon (gal)
liter (L)	61.02	cubic inch (in3)
	Flow rate	
cubic meter per second (m3/s)	35.31	cubic foot per second (ft3/s)
	Mass	
gram	0.03527	ounce avoirdupois
nanogram	3.527e-11	ounce avoirdupois

Temperature in degrees Celsius (°C) may be converted to degrees Fahrenheit (°F) as

$$°F = (1.8 \times °C) + 32.$$

Datum

Horizontal coordinate information is referenced to the North American Datum of 1983 (NAD 83).

Supplemental Information

Specific conductance is given in microsiemens per centimeter at 25 degrees Celsius (µS/cm at 25 °C).

Concentrations of chemical constituents in water are given in either milligrams per liter (mg/L) or micrograms per liter (µg/L), or nanograms per liter (ng/L).

Abbreviations

CCSB	Cache Creek Settling Basin
DI	deionized
DOC	dissolved organic carbon
DOM	dissolved organic matter
EEMs	excitation emission matrices
EPA	U.S. Environmental Protection Agency
F	Statistical test metric
FNU	Formazin Nephelometric Units
HDPE	high density polyethylene
Hg	mercury
Hg(II)	inorganic divalent mercury
IOPs	inherent optical properties
MeHg	methylmercury
NWIS	National Water Information System
p	Statistical significance of the model
PETG	polyethylene terephthalate copolyester glycol modified
QSE	quinine sulfate equivalent
RFU	relative fluorescence units
RPM	revolutions per minute
THg	total mercury
TMDL	total maximum daily load
USGS	U.S. Geological Survey

Coagulant and Sorbent Efficacy in Removing Mercury from Surface Waters in the Cache Creek Watershed, California

By Erica R. De Parsia, Jacob A. Fleck, David P. Krabbenhoft, Kim Hoang, David Roth, and Paul Randall

Abstract

Cache Creek drains part of northern California's Coast Ranges and is an important source of mercury (Hg) to the Sacramento–San Joaquin Delta. Cache Creek is contaminated with Hg from several sources, including historical Hg and gold mines, native Hg in the soils, and active mineral springs. In laboratory experiments in a study conducted by the U.S. Geological Survey, in cooperation with the U.S. Environmental Protection Agency, the use of coagulants and sorbents to immobilize Hg in water samples from high-concentration sources in the Cache Creek watershed was investigated. Three sites were selected for the collection of surface-water samples containing high and low concentrations of particulate-associated Hg. The high-particulate Hg samples were collected from Cache Creek Settling Basin during stormflow conditions. The low-particulate Hg samples were collected from two geochemically contrasting sites during base-flow conditions (downstream from a geothermal spring and at the emergence point of a connate-water spring). Three coagulants were chosen for laboratory testing with the high-particulate sample— (1) ChitoVan™ HV 1.5 percent (shell based), (2) Ferralyte™ 8131 (ferric sulfate based), and (3) Ultrion™ 8186 (aluminum based). Each coagulant was tested at various dose amounts to determine the optimum dose rate for the high-particulate sample. The low-particulate source samples were passed through three sorbents— (1) chitosan flakes, (2) coconut shell-based activated carbon, and (3) coal-based activated carbon. In-line columns were packed with each material, and the untreated sample was passed through each column at three different flow rates (0.1, 0.5, and 1.0 liter per minute, L/min).

For dose rates used in this study, ChitoVan™ reduced turbidity of the particulate sample by 85–91 percent, Ferralyte™ reduced turbidity by 54–93 percent, and Ultrion™ reduced turbidity by greater than 90 percent. At the lowest dose rate, ChitoVan™ achieved a 59- to 61-percent reduction in whole-water methylmercury (MeHg) concentrations and a 71- to 75-percent decrease in whole-water total mercury (THg) concentrations. Ferralyte™ achieved a 37- to 48-percent decrease in whole-water MeHg concentrations and a 37- to 48-percent reduction in whole-water THg concentrations. Ultrion™ achieved a greater than 90-percent decrease in whole-water MeHg and THg concentrations.

Mercury removal from the low-particulate samples was less efficient for the sorbent materials compared to the coagulants; less than 30 percent of THg was removed from any 500-milliliter aliquot using sorbent materials. The coal-based sorbent was the most versatile of the sorbents, removing THg to a similar extent from both low-particulate source waters. The chitosan sorbent was the most effective at removing THg from the low-particulate stream sample, but less effective for the low-particulate connate-spring sample. The Hg removal efficiency of the coconut sorbent decreased quickly compared to the other two sorbents, indicating that sorption may be limited by the short contact times evaluated in this study.

Introduction

Mercury (Hg) is a potent neurotoxin that affects the reproductive success, neurological development, and survival rates of a wide variety of life forms (Morel and others, 1998; Wiener and others, 2003). Methylmercury (MeHg) is the form of Hg that biomagnifies through aquatic food chains and thus poses a health risk to wildlife and humans (Wiener and others, 2003). Inorganic divalent mercury [Hg(II)] can be transformed into MeHg by sulfate- and iron-reducing bacteria that inhabit aquatic sediment and wetlands (Gilmour and others, 1992; Fleming and others, 2006; Kerin and others, 2006). Aquatic environments, especially wetlands, typically have biogeochemical conditions that are conducive to MeHg production (Hurley and others, 1995; St. Louis and others, 2004; Hall and others, 2008). Thus, aquatic environments worldwide are an important nexus between the occurrence of Hg(II) and MeHg exposure to humans and wildlife (Driscoll and others, 2013).

Because Hg(II) methylation occurs in specific aquatic habitats, the transport of Hg(II) to these habitats is important to the effective management of the MeHg threat to humans and wildlife. Mercury contamination of aquatic ecosystems is globally extensive because of natural and anthropogenic Hg emissions and transport through the atmosphere (Driscoll and others, 2013). At more localized scales, hydrologic or atmospheric transport of Hg from legacy mining sources, such as waste rock and tailings piles, mine adit drainage, and processing equipment, can increase localized Hg loadings and MeHg concentrations in local and downstream food webs (Gray and others, 2000; Rytuba, 2000; Gray, 2003; Alpers and others, 2016; Fleck and others, 2016).

The Cache Creek watershed in northern California's inner Coast Ranges provides a model watershed for studying the control of Hg mobilization in a catchment with extensive areas of sensitive habitats downstream (fig. 1). The high levels of Hg in the watershed sediment are from natural background geologic sources that could have been exacerbated by mining activities. Mercury transport from the watershed affects a diverse range of habitats from riverine floodplains in the Yolo Bypass to estuarine and coastal wetland habitats in the Sacramento–San Joaquin Delta and San Francisco Bay. The characteristics of the Cache Creek watershed are representative of many mining-affected watersheds across the western United States and throughout the world where gold and Hg mining have occurred, making it a prime candidate for studies aimed at controlling the transport of Hg downstream. The U.S. Geological Survey (USGS) in cooperation with the U.S. Environmental Protection Agency (EPA), conducted a study of the use of coagulants and sorbents to control Hg in surface water, specifically in the Cache Creek watershed. The purpose of this study was to demonstrate the utility of coagulants and sorbents by removing Hg from the waters with high-Hg levels in the Cache Creek watershed. Mercury-source types evaluated in this study included (1) particulate Hg(II) associated with fine-grained sediment and (2) filter-passed Hg(II) bound up in the dissolved and colloidal fractions.

Purpose and Scope

The purpose of this report is to summarize the results of laboratory experiments investigating the efficacy of coagulation and sorbent techniques in removing Hg from surface waters. Data in this report characterize source-water and post-treatment samples. Primary analytes include total mercury (THg), methylmercury (MeHg), and trace metals (table 1) in non-filtered water; standard water-quality measurements taken in the field at the time of sample collection and during the laboratory experiments (pH, specific conductance, and turbidity); dissolved organic carbon (DOC); and selected inherent optical properties (IOPs).

The scope of the study is limited to laboratory evaluations of the potential for the removal of Hg from Cache Creek surface water using selected materials as a proof of concept and prioritization for future research; and ultimately the application could be tested in a field-based setting. The USGS recently investigated the use of coagulation techniques in high-DOC waters on Twitchell Island in the Sacramento–San Joaquin Delta. Results indicate that effective Hg removal could be achieved in the low-particulate samples using low-dose, in situ treatment techniques (Ackerman and others, 2015; Stumpner and others, 2015). The coagulation-removal strategy is effective because it has been shown that Hg(II) and MeHg in surface waters of freshwater ecosystems are predominantly associated with dissolved and particulate organic matter (Henneberry and others, 2011). Thus, by injecting a coagulant that effectively removes much of the organic matter from water, the associated Hg species also are removed. However, little is known about the effectiveness of coagulation for the removal of Hg from waters with characteristics of either elevated particulate Hg or elevated dissolved and colloidal Hg from geothermal sources and groundwater-seepage sources. This study reflects the first step in addressing these unknowns at the bench scale before moving forward with more expansive field-scale efforts.

Methods and Materials

Methods presented in this report describe the use of coagulants and sorbents as a means of removing Hg from areas of high-Hg concentration in the Cache Creek watershed. In this section we describe the selection of sampling sites, coagulants, and sorbents tested; the collection of samples; and sample processing.

Site Selection

The Cache Creek watershed has concentrations of Hg elevated above background conditions that are derived from several sources, including historical Hg mines, historical gold mines where Hg was used for amalgamation, soils with a high natural background of Hg from hydrothermal activity, and active mineral springs (Rytuba, 2000; Churchill and Clinkenbeard, 2003; Domagalski and others, 2003, 2004a, 2004b; Rytuba and others, 2011). Sampling locations of source waters in the Cache Creek watershed were selected through a review of the literature and existing data concerning Hg contamination and associated surface-water chemistry for the watershed, pH, specific conductance, and other chemical characteristics that define different sources and reactivity (table 2).

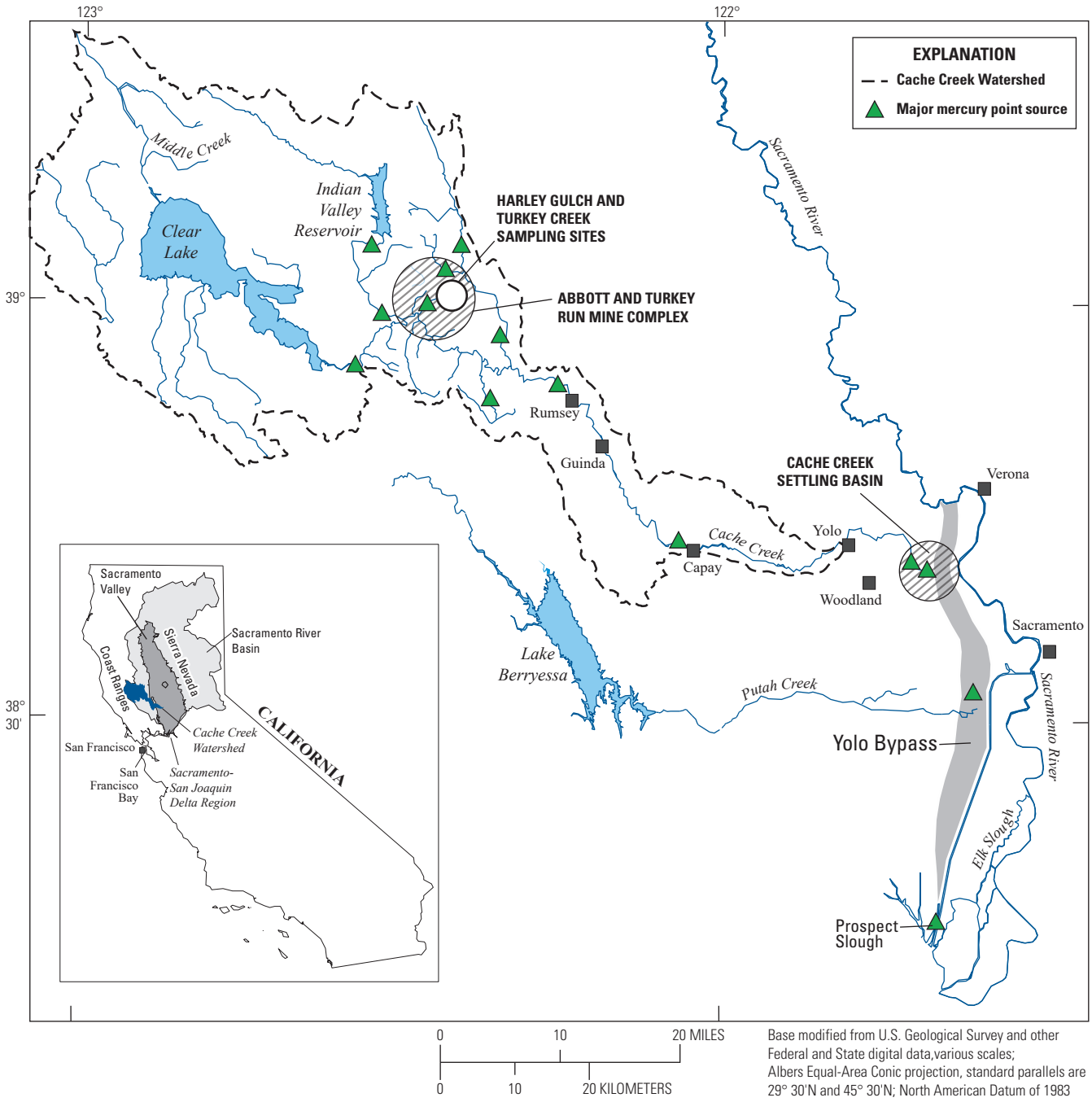

Figure 1. Cache Creek watershed showing locations of important mining features, and the Cache Creek Settling Basin and its connection to the Sacramento–San Joaquin Delta via the Yolo Bypass (modified from Domagalski and others, 2004b). Sampling sites shown in the figure represent sites used during the Domagalski and others (2004b) study.

Table 1. Selected trace metals found in whole-water samples.

Name	Abbreviation	Name	Abbreviation
Aluminum	Al	Sodium	Na
Arsenic	As	Niobium	Nd
Boron	B	Nickle	Ni
Barium	Ba	Phosphorus	P
Beryllium	Be	Lead	Pb
Bismuth	Bi	Praseodymium	Pr
Calcium	Ca	Rubidium	Rb
Cadmium	Cd	Sulfur	S
Cerium	Ce	Antimony	Sb
Cobalt	Co	Selenium	Se
Chromium	Cr	Silicon	SiO_2
Copper	Cu	Samarium	Sm
Dysprosium	Dy	Strontium	Sr
Erbium	Er	Terbium	Tb
Europium	Eu	Tellurium	Te
Iron	Fe	Thorium	Th
Gallium	Ga	Titanium	Ti
Gadolinium	Gd	Thallium	Tl
Holmium	Ho	Thulium	Tm
Potassium	K	Uranium	U
Lanthanum	La	Vanadium	V
Lithium	Li	Yttrium	Y
Lutetium	Lu	Ytterbium	Yb
Magnesium	Mg	Zinc	Zn
Manganese	Mn	Zirconium	Zr
Molybdenum	Mo		

Table 2. Field water-chemistry data, laboratory mercury, and dissolved organic-carbon data for candidate sources in the Cache Creek watershed, California.

[Sites labeled as "This study" were sampled to determine their candidacy for use in the coagulant and sorbent experiments. Sites 11452600 and 11452900 were sampled by the Cache Creek Settling Basin project and used in the coagulation full experiment. Data from the U.S. Geological Survey stations are available from the National Water Information System (NWIS, https://waterdata.usgs.gov/nwis/). **Abbreviations**: C, creek; DOC, dissolved organic carbon; FNU, Formazin Nephelometric Turbidity; fTHg, filter-passed total mercury; ID, identification; mg/L, milligrams per liter; mm/dd/yyyy, month/day/year; N/A, not applicable; ng/L, nanograms per liter; nr, near; pTHg, particulate total mercury; Trib, tributary; USGS, U.S. Geological Survey; uTHg, unfiltered total mercury; *, measured as total organic carbon; —, no data exist; [], USGS parameter code; ~, approximately; ^, estimated from field fluorescence measurements; `, North American Datum of 1983 (NAD83) coordinate system; µS/cm, microsiemens per centimeter; <, less than]

Source	Sampled (mm/dd/yyyy)	USGS station ID	Latitude	Longitude	pH	Specific conductance (µS/cm)	Turbidity (FNU)	DOC (mg/L)	uTHg (ng/L)	fTHg (ng/L)	pTHg (ng/L)	Citation
Cache C Inflow to Settling Basin nr Yolo CA	03/17/2016	11452600	38.726015`	–121.729963`	8.1 [00400]	391 [00095]	480 [63680]	—	—	1.93	96.5	Alpers oral commun., 2017
Cache C Outflow from Settling Basin nr Woodland CA	03/17/2016	11452900	38.678515`	–121.672739`	7.92 [00400]	384 [00095]	210 [63680]	—	—	2.81	30.4	Alpers oral commun., 2017
Connate Spring A Unnamed Trib nr Wilbur Springs CA	11/16/2015	390041122260401	39.011317`	–122.434350`	8.01 [00400]	6,820 [00095]	1 [63680]	~15^	131	—	—	This study
Turkey C nr Wilbur Springs CA	11/16/2015	390057122262501	39.015789`	–122.440267`	8.37 [00400]	8,250 [00095]	3 [63680]	~5^	113	—	—	This study
Turkey Creek	05/24/1994	N/A	39.016058	–122.439412	8.3	—	—	16*	—	1,100	1,600	Goff and others, 2001
Turkey Creek	02/14/2000	N/A	39.016589	–122.440076	—	—	—	—	404	—	—	Suchanek and others, 2002
Turkey Creek	02/21/2001	N/A	39.016589	–122.440076	—	—	—	—	87	—	—	Suchanek and others, 2002
Turkey Run Geothermal Spring nr Wilbur Springs CA	11/16/2015	390101122262501	39.016922`	–122.440234`	6.7 [00400]	8,560 [00095]	15 [63680]	~5^	3.1		—	This study
Turkey Run Geothermal Spring	05/24/1994	N/A	39.017489	–122.439444	6.5	—	—	<2*	—	<200	—	Goff and others, 2001
Turkey Run Geothermal Spring	02/14/2000	N/A	39.017108	–122.440201	—	—	—	—	4	—	—	Suchanek and others, 2002
Turkey Run Geothermal Spring	02/21/2001	N/A	39.017108	–122.440201	—	—	—	—	6	—	—	Suchanek and others, 2002
Downstream from Turkey Run	06/16/2010	N/A	39.0154	–122.44023	8.06	7,820	—	2.7	825	—	—	Rytuba and others, 2011
Downstream from Turkey Run	05/25/2011	N/A	39.01627	–122.44001	8.2	2,270	—	9.23	624	—	—	Rytuba and others, 2011
Middle of Harley Gulch Wetland	05/25/2011	N/A	39.01402	–122.43709	8.26	5,560	—	4.66	2,300	—	—	Rytuba and others, 2011

Four sites were selected and sampled for the experiments described in the following subsections of this report. Two locations in the Cache Creek Settling Basin (CCSB) were selected for the particulate-dominated Hg sample (Cache Creek Inflow to Settling Basin near Yolo, CA; 11452600 and Cache Creek Outflow from Settling Basin near Woodland, CA; 11452900). The CCSB is a sedimentation basin located where Cache Creek empties into the Yolo Bypass en route to the San Francisco Bay (fig. 1). The water entering the CCSB is an integration of all the upstream sources, and the Hg transport is dominated by suspended sediment from mine-affected and natural landscapes across the watershed (Cooke and others, 2004; Foe and Bosworth, 2008; C.N. Alpers, U.S. Geological Survey, written commun., 2017). Two locations in the Harley Gulch area downstream of the Abbott and Turkey Run Mine complex (fig. 1) were selected for the low-particulate Hg sampling. One site (Turkey Creek near Wilbur Springs, CA; 390057122262501) is approximately 100 meters (m) downstream of a geothermal spring. The other site (Connate Spring at Unnamed Tributary near Wilbur Springs, CA; 390041122260401) is at the emergence point of a connate-water spring. The low-particulate samples have sources and chemical characteristics like those collected by Rytuba and others (2011). The two low-particulate sites selected for this study (390041122260401 and 390057122262501) had similarly high-Hg concentrations but differed in other chemical characteristics (table 2), with mercury most likely existing in the dissolved and colloidal forms.

Coagulant and Sorbent Selection

The selection of coagulants and sorbents for the laboratory experiments was accomplished through literature review and consultation with coagulant manufacturers and stormwater-treatment professionals. The effectiveness of coagulant and sorbent types is dependent on the physical and chemical characteristics of the water to be treated (table 3). Three coagulants were selected for testing the high-particulate samples. ChitoVan™ HV 1.5 percent (Dungeness Environmental Solutions Inc., Bothell, Washington) is a liquid form of chitosan acetate (proprietary blend) derived from natural source materials (crab and shrimp shells) used commonly in stormwater treatment. It has been extensively tested for release into the environment (Macpherson, 2004) and has been used as a plant growth enhancer (Freepons, 1997). Ferralyte™ 8131 (NALCO, Naperville, Illinois) is a ferric sulfate (proprietary blend) based solution used primarily in wastewater and raw-water clarification, odor control (hydrogen sulfide), and phosphate removal. Ultrion™ 8186 (NALCO, Naperville, Ill.) is a high activity, high-molecular weight, aluminum-based (proprietary blend) cationic coagulant used for paper, wastewater, and drinking-water processing. Ultrion™ is available in high and low concentrations; the low concentration was used for this study.

Coagulants selected for the low-particulate Hg sources were the same as for the high-particulate source except for the ChitoVan™ coagulant. Preliminary tests indicated the ChitoVan™ coagulant was unlikely to be effective on the low-particulate sources, so a metal scavenging co-precipitant (MetClear™ 2405; GE Water and Process Technologies, Trevose, Pennsylvania) was selected as a replacement for ChitoVan™. This metal scavenger is less environmentally friendly than the coagulants but may be effective in a more actively managed system for the mercury speciation encountered in these systems.

Sorbents also were selected for the low-particulate Hg sources because there was uncertainty that the coagulation process would be successful in removing Hg not associated with dissolved organic matter (DOM) or particles (Henneberry and others, 2011). The selected sorbents included two forms of activated carbon, one made from charred coconut husks and one derived from mined coal (Carbon Activated Corp., Compton, California), and the third sorbent is made from solid-phase chitosan flakes (Dungeness Environmental Solutions Inc., Bothell, Wash.). All sorbents were sieved (less than 1 millimeter [mm]). Sorbents were not evaluated for the high-particulate source samples.

Procedures

The experiments focused on two types of Hg-source samples: (1) high-particulate, with Hg predominately bound up in fine-grained suspended sediment (C.N. Alpers, U.S. Geological Survey, oral commun., 2017), and (2) low-particulate, with Hg predominantly present in the dissolved and colloidal fractions that pass through a 0.45-micron filter (Rytuba and others, 2011). The coagulation experiment was done in two phases to maximize success because the experiment demanded large volumes of water to do the testing, and the streaming current detector was out of operation during the critical wet, raining period when sampling was required. A streaming current detector is a device that measures the stability of coagulant particles in water (Sibiya, 2014). The first phase involved a coagulation "**test run"** in which a large volume (605–609 milliliters, mL) of a turbid sample was dosed with ChitoVan™ to determine the approximate scale of optimal dose for all three coagulants using turbidity as an analog for Hg removal. The second phase used the results from the first phase to complete the coagulation "**full experiment"** on a freshly collected large-volume sample. Coagulants were tested on both sample types.

Table 3. Site characteristics affecting the effectiveness of coagulants and sorbents.

[Ca2+, calcium; DOC, dissolved organic carbon; Hg, mercury; mg/L, milligram per liter; mmol, millimole; nmol, nanomole; ° C, degrees Celsius; >, greater than; <, less than; —, not applicable]

Site characteristic	Effect on coagulation and sorption treatments	Notes	Citation
pH	Changes in pH may negatively affect coagulation efficiency as it can result in unintentional shifts in the coagulation-flocculation mechanism, potentially causing charge reversal and re-suspension of particles. Also, with redox status, affects chemical speciation and stability.	Acceptable ranges for floc formation: –5.5 to 7.5 = alum optimal range –5.0 to 8.5 = ferric salts optimal range pH> 8.5 = ferric salts or other highly acidic coagulants recommended	Haitzer and others, 2003; Bratby, 2006
Alkalinity/salinity/ ionic strength/ condictivity	**LOW**: <50 mg/L alkalinity is too low for salt-based coagulants; adding lime, soda, ash or caustic as an aid is recommended. **HIGH:** Halogen-dominated and high cation (Ca^{2+}) systems affect Hg-binding and may make the coagulant ineffective.	Coagulation aids for LOW alkalinity conditions may raise the pH of the water; pH adjustment may be needed to obtain proper floc formation.	Bratby, 2006
Temperature	Coagulation becomes less efficient in cold temperatures. Higher coagulant doses must be used to compensate.	Temperature <5 °C = alum and ferric salts may not provide proper floc formation at low temperatures (<5 °C)	Bratby, 2006
Particle concentration	**LOW**: difficult to coagulate due to the difficulty of inducing collision between the colloids. **HIGH**: dose requirement becomes challenging to meet.	—	Bratby, 2006
Particle type	Clays and negatively charged colloids respond well to metal salt-based coagulants.	The types of particles affect dose requirements, though not in a linear manner.	Bratby, 2006
DOC concentration	DOC consumes coagulant. May reduce effectiveness of particulate removal or enhance removal of dissolved species.	—	Henneberry and others, 2011
DOC - Hg ratio	High Hg = DOC have lower binding strength which may lower coagulant effectiveness.	Ratios <120 nmol Hg:mmol DOC are strong binding sides Ratios >120 nmol Hg:mmol DOC are weaker binding sites	Haizer and others, 2002, 2003
Redox conditions	If applies to environment in situ, redox status may be important to both the coagulation process and floc stability. Effects are complex and dependent on coagulant type and other environmental variables coupled with the redox state.	Strongly reducing conditions may inhibit coagulation and floc formation using iron-based flocs if the iron is converted to a mobile, soluble phase, or it may enhance floc stability and limit Hg bioavailability if insoluble, solid-phase iron species form.	Benoit and others, 2001; Henneberry and others, 2012
Total metals/cation concentration	High concentrations of cations may compete with the binding/ adsorption of the target mercury species and require more coagulant or more sorbent surface area to be effective.	—	Langner, 2009
Delivery/mixing	Poor site characteristics that limit sufficient transport, or inadequate mixing, will result in a variety of problems.	—	Bratby, 2006

Part 1: High-Particulate Sample Mercury Removal

Sample Collection

Two large volume samples were collected from the CCSB during March 2016— (1) one for an initial test of the coagulants and (2) one for a full experimental run with the coagulants (fig. 2)—following mercury clean-sampling protocols (U.S. Geological Survey, 2012). The first sample was collected at the inlet to the CCSB (11452600) during the first storm on March 6, 2016, which exceeded the targeted 3,000 cubic feet per second (ft^3/s) threshold at Cache Creek at Yolo (fig. 2). A total of 20 liters (L) of high-turbidity water at 1,308 Formazin Nephelometric Units (FNU) were collected in two Teflon™-lined 12-L jerricans at the inlet of the CCSB, in coordination with ongoing Hg sampling at this location (C.N. Alpers, U.S. Geological Survey, oral commun., 2017). The sample was collected on the rising limb of the hydrograph and used for the initial test run of the coagulants. The second sample was collected on March 17, 2016, at the inlet and outlet (11452600 and 11452900, respectively) of the CCSB on the falling limbs of the hydrographs and used for the coagulation full experiment one week later. Two 10-L samples were collected at each site for a total of 40 L. Turbidity at the inlet (11452600) was 500 FNU, and turbidity at the outlet (11452900) was 238 FNU, which represent much lower turbidity values compared to the value for the original test sample (1,308 FNU). Because of a forecast for an extended drought, it was likely that no further samples would be collected for the experiment, so the samples from the two sites were composited to create a single, homogenous turbid sample for the coagulation experiment rather than being tested as two independent samples. The composited sample used in the full experiment had an average laboratory turbidity value of 342 FNU.

Coagulation Jar Tests

For the coagulation test run, the initial dosing rates were determined by literature review, suggestions from experienced stormwater technicians, and the "test run." The initial dose rates were then adjusted through experimentation before being used on the coagulation full experiment. A dose range from 20 to 120 microliters (µL) of a 1.5-percent solution of ChitoVan™ was selected for the experimental run to cover the range of greatest change in turbidity encountered in the test runs. The experimental dose range was selected to determine the optimal dose rate, which is the rate with the greatest turbidity decrease per unit of dose material on the dose-response curve. Dose amounts lower than 20 µL were not tested because of accuracy limits of the dosing equipment used in the experimental set up.

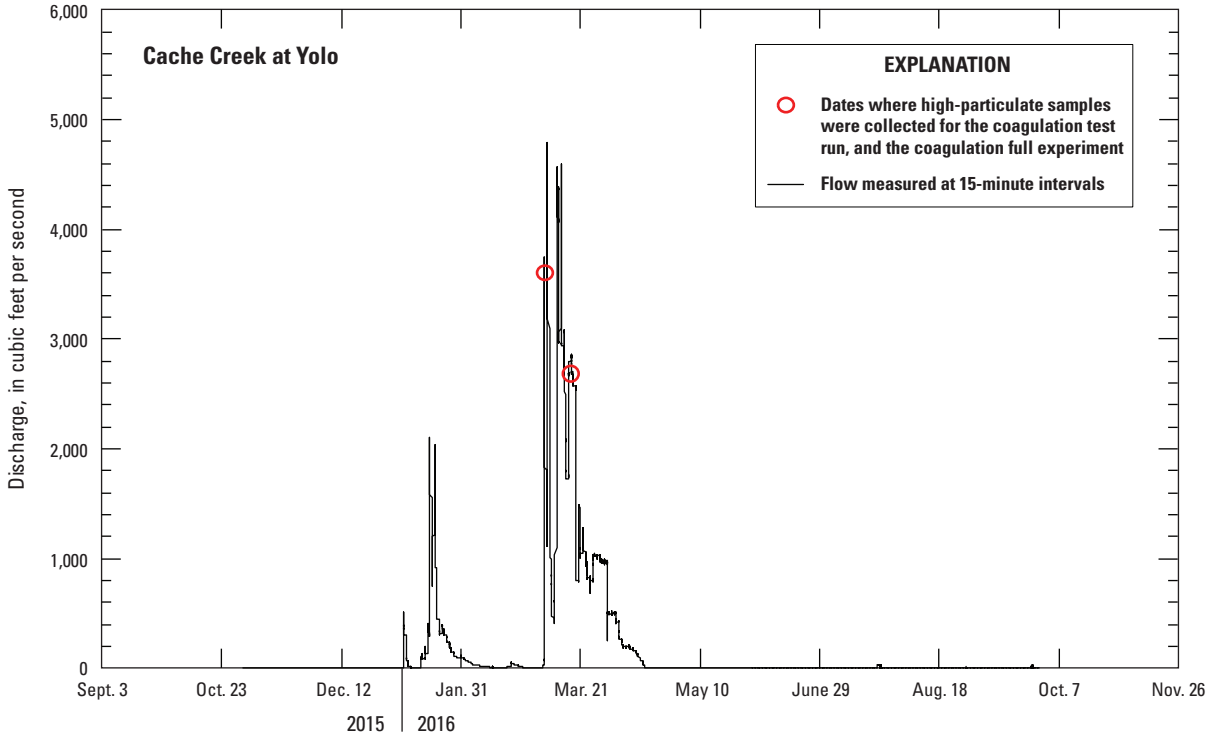

Figure 2. Flow conditions at the time when the high-particulate samples were collected relative to the flows over the hydrologic year. The targeted flow rate for sample collection was greater than 3,000 cubic feet per second. Flow data were obtained from the U.S. Geological Survey real-time monitoring station, Cache Creek at Yolo, California (https://waterdata.usgs.gov/nwis/uv?11452500), which is approximately 13 kilometers upstream of the sampling location, Cache Creek Inflow to Settling Basin near Yolo CA (11452500).

The coagulation full experiment was done in two stages: (1) a "dirty" run in glass beakers, allowing for collection of ancillary (non-Hg) water-quality measurements and (2) a "clean" run, enforcing Hg clean techniques and allowing for Hg-specific sample collection. The three coagulants were tested in the following order (1) ChitoVan™, (2) Ferralyte™, and (3) Ultrion™. Four 12-L Teflon™-lined jerricans of samples were collected at the locations described above. One jerrican from each site was composited into a 20-L Teflon™-lined churn. Jerricans were vigorously shaken before emptying into the churn. After completion of the first coagulant test, 5 L from each of the two remaining jerricans was composited into the same churn to ensure that enough volume was present to complete testing of the second coagulant. The third coagulant was tested 4 days after the first test, and the remaining sample in each jerrican was agitated and composited into a clean 20-L Teflon™-lined churn.

For the "dirty" stage of the experiment, six clean glass beakers were labeled with the coagulant used and the corresponding dose amount. Each beaker was tared and filled with 966–1,000 mL of the sample. The beakers were re-weighed to determine the exact amount of water added and placed on a magnetic stir plate set to 600 revolutions per minute (RPM). Before the coagulant addition, turbidity, pH, fluorescent DOM, and specific conductance measurements were collected from each jar using a YSI EXO2 water-quality sonde (YSI, Yellow Springs, Ohio); total water-column depth also was measured. Each beaker was dosed with the specified amount of coagulant (table 4). ChitoVan™ and Ferralyte™ were mixed for 2 minutes. However, upon further inspection it was determined that 2 minutes was not enough mixing time for the full amount of flocculant to form, so mixing time was increased to 5 minutes for the "dirty" stage of Ultrion™ and the "clean" stage for all three coagulants. After mixing, the beakers were removed from the stir plates and beaker-specific timers were started to record the flocculant settling time. Measurements of the above listed characteristics were taken after 5, 10, 20, and 30 minutes of settling. At each time point, the visual depth of the overlying water column was recorded, and the clarity of the overlying water column was visually noted. Once the 30-minute measurements were completed, the overlying water of the coagulant-amended beakers was gently poured off to minimize disturbance, and the remaining flocculant was composited and poured off into 20-mL scintillation vials that were subsequently used for grain-size distribution analysis or were archived (frozen).

The "clean" experiment was repeated with six 1-L polyethylene terephthalate copolyester glycol modified (PETG; Thermo Fisher Scientific, Waltham, Massachusetts) bottles; four bottles received a specified dose (table 4) across the range determined from the "dirty" dosing curve, one control bottle received no dose, and one bottle was filled with organic-free water as the blank (fig. 3). Each bottle was labeled with the coagulant used and corresponding dose amount, and then tared and filled with approximately 1-L of sample water. The bottles were re-weighed to determine the exact amount of water added and placed on a magnetic stir plate set to 600 RPM. Each bottle was dosed with the specified amount of coagulant and allowed to mix for 5 minutes. After 5 minutes of mixing, the bottles were removed from the stir plates and bottle-specific timers were started to record flocculant settling time. The visual depth of the clarified water column was measured every 5 minutes up to 25 minutes and then again at 40 minutes (fig. 3). A Masterflex™ peristaltic pump and Teflon™ sampling line were used to pump the overlying clarified water into 1-L PETG bottles without disturbing the flocculated materials. The water sample was then homogenized by shaking immediately before pouring the sub-sample splits identified below.

Each 1-L sample was split into two 125-mL PETG bottles for MeHg and THg analysis, one 250-mL high-density polyethylene (HDPE) bottle for trace-metal analysis (if needed), and one 125-mL amber-glass bottle for optical properties and DOC analysis; the remaining volume went into a glass scintillation vial for analysis on a benchtop turbidity meter (Hach 2100AN IS Turbidimeter, Loveland, Colorado) using the shake and pour method. Mercury samples were preserved to 1 percent by volume with concentrated hydrochloric acid. Trace-metal samples were preserved with 2 mL of quartz-distilled nitric acid. Optical property samples were poured into Teflon™ filter towers and vacuum filtered through pre-combusted 0.3-micron glass-fiber filters (GF75 47 mm; Advantec MFS, Inc., Dublin, Calif.) and collected in 125-mL amber-glass bottles. Optical-property analyses were performed within 2 days of sample collection and filtration. Dissolved organic carbon samples were poured off from the amber-glass bottles, acidified to less than 2 pH with concentrated sulfuric acid, and refrigerated for no more than 28 days before DOC analysis.

Table 4. Summary table listing the coagulants and sorbents used in this experiment. Source samples tested, dose amounts, and flow rates used with each coagulant and sorbent also are shown.

[Coagulation "test run" information is not shown. **Abbreviations**: L, liters; L/min, liters per minute; TM, trademark; µL, microliters; %, percent]

Coagulants selected	Source sample tested	Dose amounts tested (µL)
ChitoVan™ HV 1.5%	high-particulate, low-particulate	20, 30, 50, 120
Ferralyte™ 8131	high-particulate, low-particulate	20, 40, 60, 100
Ultrion™ 8186	high-particulate, low-particulate	20, 40, 60, 100

Sorbents selected	Source sample tested	Flow rates tested (L/min)	Total amount of water tested per flow rate (L)
chitosan (shell-based)	low-particulate	0.1, 0.5, 1.0	3
coconut-based activated carbon	low-particulate	0.1, 0.5, 1.0	3
coal-based activated carbon	low-particulate	0.1, 0.5, 1.0	3

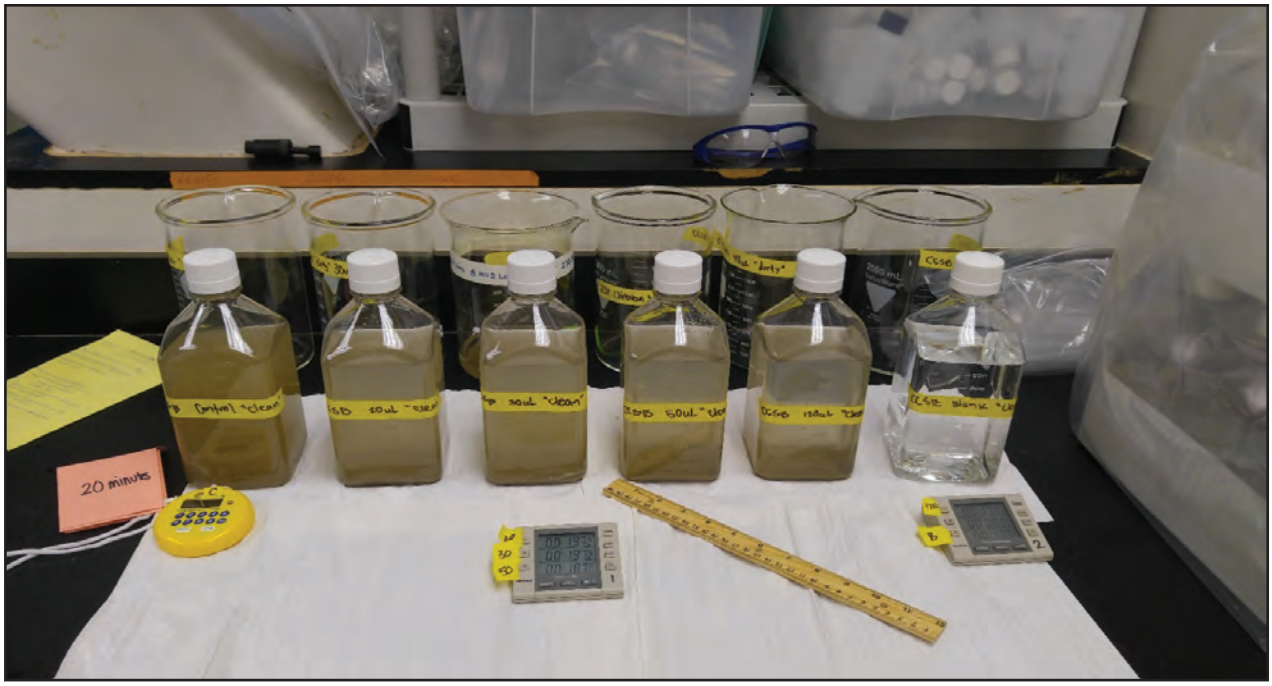

Figure 3. Bottles from the coagulant dosing series for ChitoVan™ after 20 minutes of settling. Coagulant amendment amounts increase from left to right; the blank at the right end.

Part 2: Low-Particulate Sample Mercury Removal

Sample Collection

The removal of Hg species (MeHg and THg) by coagulation and sorption was tested on samples collected during base-flow conditions from two locations in the Harley Gulch area (390041122260401; 390057122262501) as described previously; site 390057122262501 was sampled during low-flow conditions. At each site, on May 3, 2016, a large volume of water was collected into a 10-L Teflon™-lined jerrican following trace-metal sampling protocols (U.S. Geological Survey, 2012). The samples were collected at the surface, and the contribution of dissolved gaseous Hg is assumed to be negligible.

Coagulation Jar Tests

Coagulants and the metal scavenging agent were tested on water samples from each site, following methods like those for the high-particulate Hg samples from the CCSB with slight modifications. Sequential coagulant dosing of unfiltered-water samples from the Turkey Creek site (390057122262501) was used during the test run instead of separate bottles for each coagulant dosing level. Visual inspection of flocculant material production was used as a measurement of success, rather than measuring the loss of turbidity. Because visible flocculant material was not produced for the non-filtered water sample, three sorbents were tested as an alternate approach to Hg removal. An aliquot was collected from each sample for determination of optical properties and for DOC analysis to characterize differences in the dissolved phase between the two source waters before treatment. Optical property samples were poured into Teflon™ filter towers, gravity filtered through pre-combusted 0.3-micron glass-fiber filters (GF75 47 mm; Advantec MFS, Inc., Dublin, Calif.), and collected in 125-mL amber-glass bottles. All samples were placed on ice in a dark cooler until delivered to the laboratory where they were transferred to a refrigerator. Optical-property analyses were performed within 2 days of sample collection and filtration. Dissolved organic carbon samples were poured off from the amber-glass bottles, acidified to less than 2 pH with concentrated sulfuric acid, and refrigerated for no more than 28 days before DOC analysis.

Sorbent Experiments

The three selected sorbents were tested over the course of 2 days in the following order (1) chitosan flake, (2) coconut-based activated carbon, and (3) coal-based activated carbon. Sample water was collected from the two Harley Gulch area sites (390041122260401; 390057122262501) via a peristaltic pump into Teflon™-lined jerricans using Hg clean techniques (Wilde and others, 2004). The chitosan flake and coconut-based activated carbon sorbents were tested on May 4, 2016, and the coal-based activated carbon sorbent was tested on May 5, 2016.

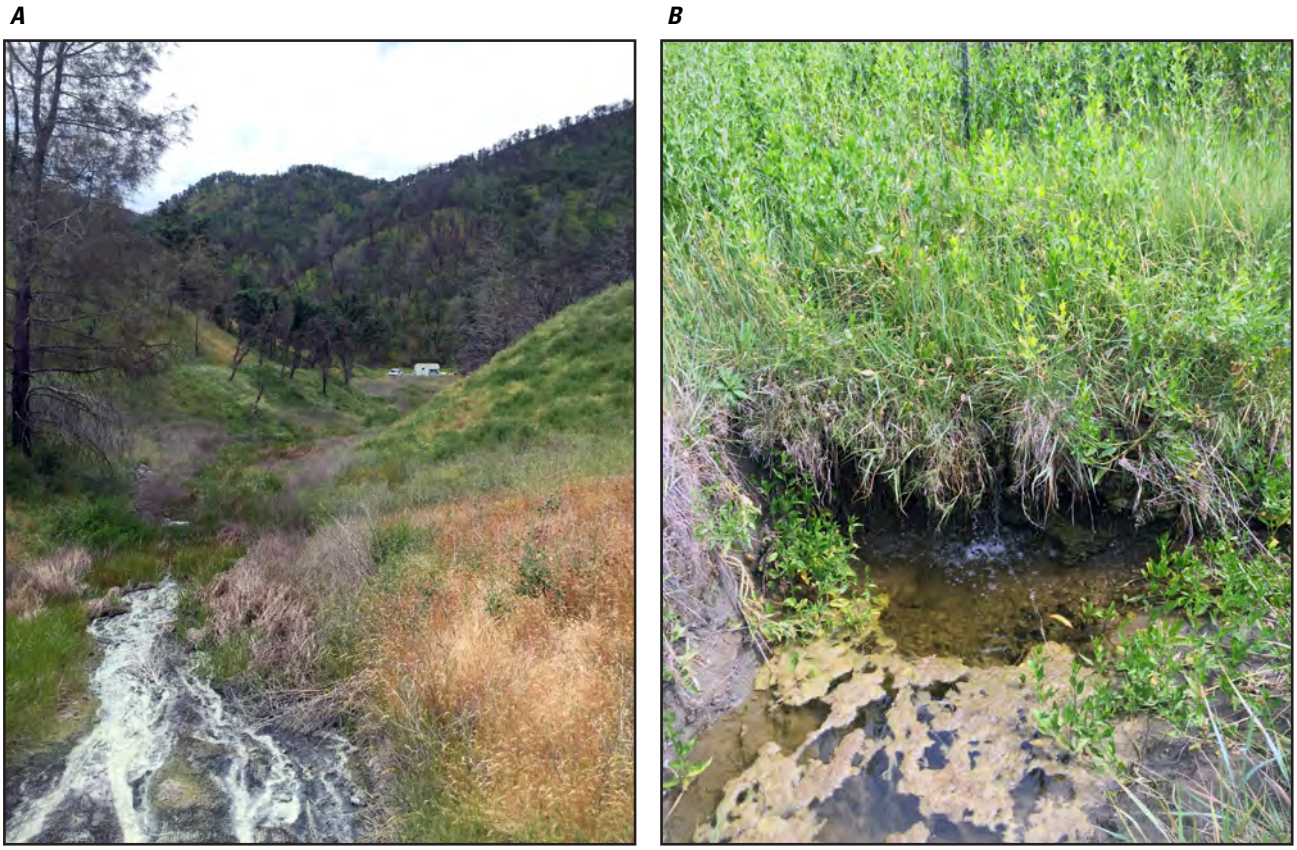

Figure 4. *A*, Turkey Creek downstream from the geothermal spring exiting the Turkey Run mine adit and *B*, the Connate Spring.

Testing of the sorbents was done on site in a mobile field laboratory (fig. 4). Each sorbent was thoroughly rinsed with deionized (DI) water in a 1-mm mesh sieve to ensure the particle size was greater than 1 mm and to remove any excess dust. Sorbent materials were prepared and packed before transportation to the field site. Teflon™ in-line filter columns were packed to the brim with each type of sorbent, and DI water was added to each packed column to ensure the sorbent was evenly distributed in the filter column. Sample water was pumped from the jerrican through the sorbent-packed columns using Teflon™ tubing. Three different flow rates were selected to be tested with each sorbent (0.1, 0.5, and 1 liter per minute [L/min]), which corresponded to contact times between sample and sorbent of approximately 10 seconds, 2 seconds, and 1 second, respectively (table 4); new columns were used for each flow rate. After passing through the in-line filter, water was collected in 500-mL increments until 3 L had passed through each sorbent filter at the three designated flow rates. A method blank also was tested by passing organic-free water through acid-cleaned glass beads.

From each 500-mL aliquot, sample splits were shaken to homogenize and poured off into 250-mL HDPE bottles for trace-metal analysis, and then into 125-mL PETG bottles for MeHg and THg analysis. Mercury samples were preserved to 1 percent by volume with concentrated hydrochloric acid. Trace-metal samples were preserved with 2 mL of quartz-distilled nitric acid. Both sets of samples were then stored in ambient temperature in the dark until further processing.

Analytical Methods

The analytical methods presented in this report were used to obtain results for samples collected during the coagulation and sorption experiment. Analytical methods used to obtain optical results and DOC, trace-metal, MeHg, and THg concentrations are detailed below.

Total Mercury and Methylmercury Concentration Analysis

Total mercury and MeHg concentrations were measured by methods like those used by Stumpner and others (2015) at the USGS Mercury Research Laboratory in Middleton, Wisconsin (appendices 1, 2). Whole-water THg concentrations were measured according to EPA Method 1631 (U.S. Environmental Protection Agency, 1999). Whole-water MeHg concentrations were measured using distillation/ethylation and gas-phase separation with cold vapor atomic fluorescence spectrometry as described by DeWild and others (2002). Method detection limits for MeHg and THg concentrations in whole-water samples were 0.04 nanogram per liter (ng/L).

Dissolved Organic Carbon Concentration and Optical Characterization of Dissolved Substances

Dissolved organic matter concentration and IOPs were analyzed at the USGS Organic Matter Research Laboratory in Sacramento, Calif. Dissolved organic matter was measured using a high-temperature combustion total organic carbon analyzer (Model TOC-V_{CHS}; Shimadzu Scientific Instruments, Columbia, Maryland) according to EPA Method 415.3 (U.S. Environmental Protection Agency, 2005). Characterization of IOPs (spectral absorbance and fluorescence) was done with an Aqualog® Spectrofluorometer (Horiba Scientific, Edison, New Jersey) using methods outlined in Hansen and others (2016).

Trace-Metal Concentration Analysis

Whole-water trace-metal concentrations were measured via inductively coupled plasma mass spectrometry at the USGS National Research Program Trace Metals Research Laboratory in Boulder, Colo. Methods used were like those of Taylor and others (2012).

Grain-Size Distribution Analysis

Particle-size distribution was measured on a composite sample of the settled material from all six doses for each coagulant using a Beckman Coulter LS™ 13–320 Laser Diffraction Particle Size Analyzer (Beckman, Brea, Calif.) equipped with an Aqueous Liquid Module, employing sonication and autodilution at the USGS Hydrologic Research Laboratory in Sacramento, Calif. Analyses were performed according to the instrument user's manual (Beckman Coulter, 2011), and data were processed according to Marineau and Wright (2017). To avoid chemically altering the size of the flocculant particles, sample bottles were shaken vigorously to re-suspend the settled material and run on the instrument without the aid of any dispersant material; however, the samples were sonicated during analysis to measure only physically stable particles. Coagulated materials were run in replicate, whereas raw-water samples had limited settled material and thus were run only once.

Coagulant and Sorbent Efficacy in Mercury Removal

Results from the high-particulate and low-particulate Hg-removal experiments are summarized independently to focus on the specific objectives of each water source and experimental approach. For the particulate-enriched water source, we focused on the coagulation experiments, whereas the sorbent experiments measured Hg removal from both the dissolved and colloidal phases.

Part 1: Particulate-Dominated Source

Coagulation Test Run

The highly turbid sample responded to the addition of the ChitoVan™ (fig. 5; appendix table 3–1). The untreated sample had a turbidity of approximately 1,300 FNU. Turbidity removal followed a curvilinear response to the dose rate, with turbidity decreasing in value as the dose rate increased. There was an 81-percent decrease in turbidity in the first 5 minutes of settling for the lowest dose rate (33 µL/L). After 10 minutes of settling, the turbidity was lowered by 85 percent and after 20 minutes, by 87 percent. For the second lowest dose rate (99 µL/L), turbidity was lowered by 97 percent after 5 minutes of settling, by 98 percent after 10 minutes, and by 98 percent after 20 minutes. Settling time had little effect on the percentage of turbidity removal; minor differences occurred after 5 minutes. The largest decrease in turbidity was at the 30-µL/L dose rate; little improvement occurred from additional dosing beyond 100 µL/L. The apparent optimal dose rate was determined to be less than 100 µL/L and possibly less than 30 µL/L; therefore, the full experiment was designed to bracket this range.

Coagulation Full Experiment

The coagulation full experiment was focused on the removal of MeHg and THg in a particulate-dominated sample but revealed marked differences in coagulant effectiveness with respect to the removal of particulate and dissolved constituents. In addition, ancillary measurements of water quality and particle character help to explain observed differences in MeHg and THg removal efficiency and the stability of the formed flocs in the environment.

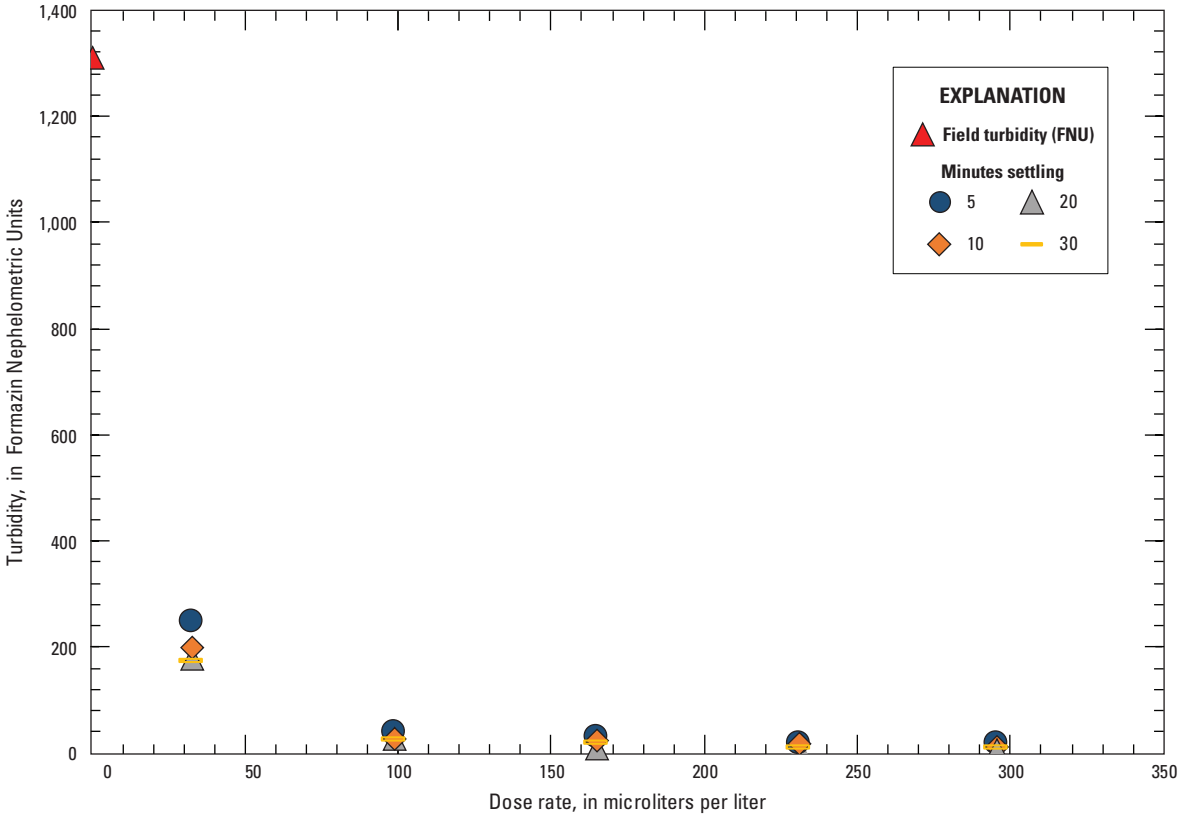

Figure 5. ChitoVan™ dose-rate turbidity response curve for the initial coagulation test run, using a storm-runoff sample. Turbidity values for each settling time were collected in the laboratory.

Mercury Removal

All coagulants effectively removed MeHg and THg from suspension in the high-particulate sample (fig. 6; appendix table 1–1). ChitoVan™ lowered the THg mean concentration by 82 percent from 37 to 6.5 ng/L at the highest dose tested (120 µL/L). The removal of MeHg, mean concentration reduced from 0.38 to 0.11 ng/L at the highest ChitoVan™ dose, was slightly less (71 percent) than THg removal. However, most of the removal of MeHg and THg occurred in the lowest dose rate tested (20 µL/L), accounting for greater than 90 percent of the removal at the 120-µL/L dose. Ferralyte™ efficacy was like that of ChitoVan™ at the highest dose amount (100 µL), removing 87 and 74 percent of MeHg and THg, respectively (fig. 6). Ferralyte™ was less effective than ChitoVan™ at lower dose rates, removing only 43 percent of MeHg and THg at the lowest dose rate (20 µL/L). Ultrion™ was the most effective at lowering MeHg and THg concentrations, achieving a greater than 90-percent decrease in MeHg species at the second lowest dose (40 µL/L), and a greater than 90-percent decrease in THg at the lowest dose (20 µL). At the lowest dose, 90-percent MeHg removal was achieved for one sample, but only 45 percent for the replicate sample. Given that this dose rate achieved 90-percent removal of both turbidity and THg in replicate, the replicate sample for MeHg is likely a result of error or contamination. An increase in the Ultrion™ dose rate did improve removal of MeHg, although that result could have been affected by MeHg measurements being very near the method detection limit.

Turbidity

ChitoVan™ was effective at decreasing the turbidity of the solution even at low-dose rates (fig. 7*A*; appendix table 3–1). The ChitoVan™ optimal dose rate appears to be between 20 and 50 µL/L for the 342 FNU sample, whereas the optimal dose rate is between 30 and 100 µL/L for the greater than 1,000 FNU sample associated with the test run. Turbidity decreased with an increase in dose rate and time after the dose. There was a 54-percent decrease in turbidity at the lowest dose rate (20 µL/L) after 5 minutes of settling, but the decrease increased to 73 percent after 30 minutes. Higher dose rates were less affected by the settling time. A dose rate of 30 µL/L led to a 71-percent decrease in turbidity after only 5 minutes of settling and increased to 78 percent after 30 minutes. Additional turbidity removal obtained from dose rates greater than 30 µL/L did not increase removal rates, indicating that these dose rates were above the optimal dose (figs. 7*A*, 7*D*).

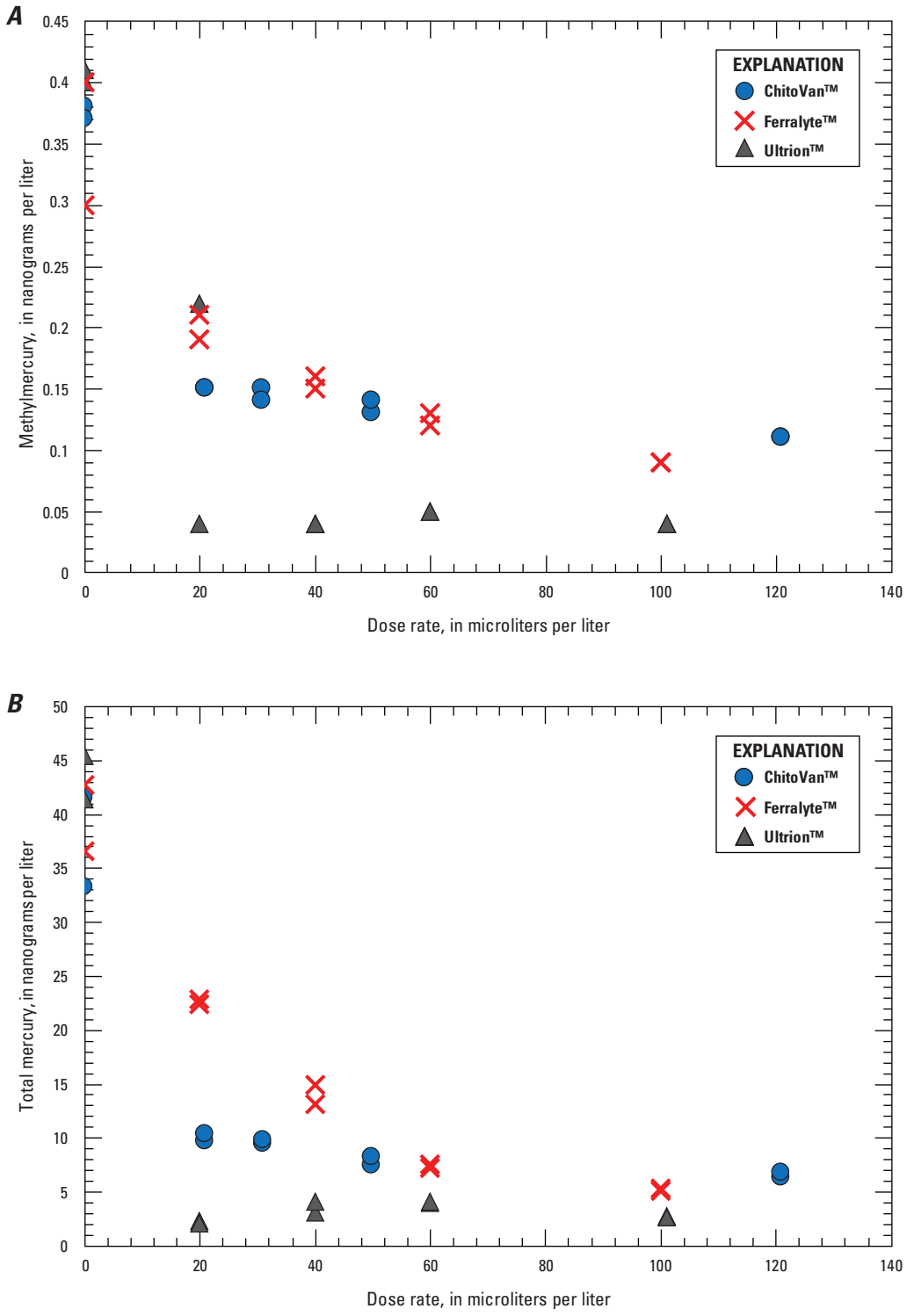

Figure 6. Decrease in *A*, methylmercury concentrations and *B*, total mercury concentrations for different dose rates during the coagulation full experiment.

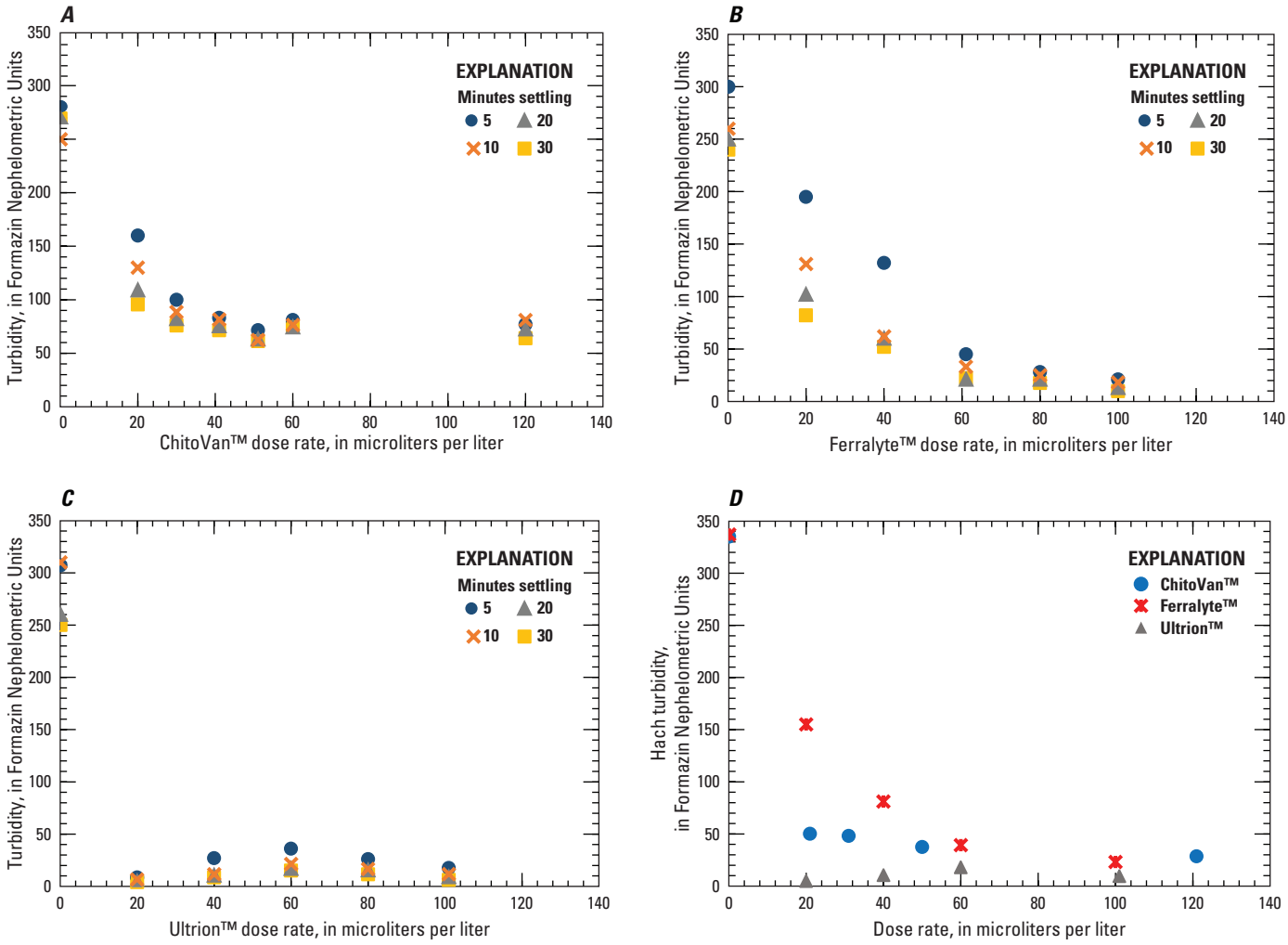

Figure 7. Coagulant dose-rate turbidity-response curves for three coagulants: *A,* ChitoVan™; *B,* Ferralyte™; *C,* Ultrion™ over time; and *D,* turbidity for all three, were measured using a Hach Turbidimeter at the end of the "clean" stage of each experiment.

Ferralyte™ required a higher dose rate than ChitoVan™ to lower the turbidity to less than 50 FNU; the optimal dose was in the range of 60–100 µL/L (fig. 7*B*). There was a 44-percent decrease in turbidity at the lowest dose amount (20 µL) after 5 minutes of settling, and a 77-percent decrease in turbidity after 30 minutes. At the 60-µL/L and higher dose rates, turbidity removal was greater than 80 percent, and the speed at which the flocs settled increased (fig. 7*B*).

Ultrion™ was most effective at decreasing turbidity at low-dose rates (fig. 7*C*). At the lowest dose rate (20 µL/L), there was a 97-percent decrease in turbidity after 5 minutes of settling. The optimal dose rate is less than or equal to the lowest dose rate (20 µL/L). There was some indication that decreasing turbidity was less effective (89–93 percent decrease) at the mid-range dose rates (30–80 µL/L), but the difference was within the error of measurement. The effectiveness at the highest dose rate (100 µL/L) was like that at the lowest dose rate (20 µL/L).

Measurements from the end of each experiment (fig. 7*D*) illustrate the differences among the coagulant efficacies in decreasing turbidity, and parallel the trends seen in MeHg and THg removal. Ultrion™ was most effective at lowering turbidity at the lowest dose rates. Ferralyte™ required the highest dose rate to lower turbidity to the 50 FNU level, and ChitoVan™ required a medium dose rate between Ferralyte™ and Ultrion™ at dose rates up to 50 uL/L. The turbidity response curve for Ferralyte™ was more incremental than for the other coagulants.

Flocculant Size and Physical Stability

The particle-size distribution of the settled material in the coagulation full experiment differed among the coagulants tested (fig. 8). The particle size of the materials treated with Ultrion™ showed the greatest difference in particle-size distribution compared to that of the raw-water materials and was dominated by medium-to-coarse silt with an average median particle size of 21 micrometers (µm; table 5). The Ultrion™ coagulant also appeared to be the most effective at aggregating the smallest particles, raising the 10th percentile of the particle size from less than 1.5 to 5 µm, and lowering the fraction as clay to less than 9 percent (fig. 8; table 5). In contrast, the Ferralyte™ and ChitoVan™ coagulants experienced a loss of particles in the 2- to 5-µm range and concomitant increase of particles in the 6- to 20-µm range, but ultimately these had a relatively small effect on the overall distribution (fig. 8). The changes in particle-size distribution despite the marked increase in settled materials likely reflects the production of unstable particles that disaggregated upon sonication. The variability in the percent of sand-size particles was attributed to the variability inherent in subsampling of the material and the inclusion of aggregates when a dispersant is not used (Beckman Coulter Inc., 2011).

Dissolved Organic Matter

Coagulants can remove DOM and the MeHg and THg associated with specific types of DOM from the water column (Henneberry and others, 2011). Changes in the optical character of the samples were assessed to better understand the differences observed in the removal of MeHg and THg associated with DOM for the different coagulants.

ChitoVan™ had little effect on DOM concentration or optical properties (figs. 9–12). ChitoVan™ caused DOC concentrations to increase slightly with each increase in dose rate, which could be attributed to the coagulant being an organic-based compound (fig. 9*A*) and had a minor effect on IOPs related to DOM character (figs. 9*B–D*). The full absorbance scans show a consistent non-linear decrease in the total absorbance of the sample with increasing wavelength (from 240 to 540 nanometers, nm) and a small overall decrease in absorbance in ChitoVan™ amended samples compared to that in untreated raw water (fig. 10*A*). There was no discernable effect from the addition of ChitoVan™ across the fluorescence spectra (figs. 11, 12).

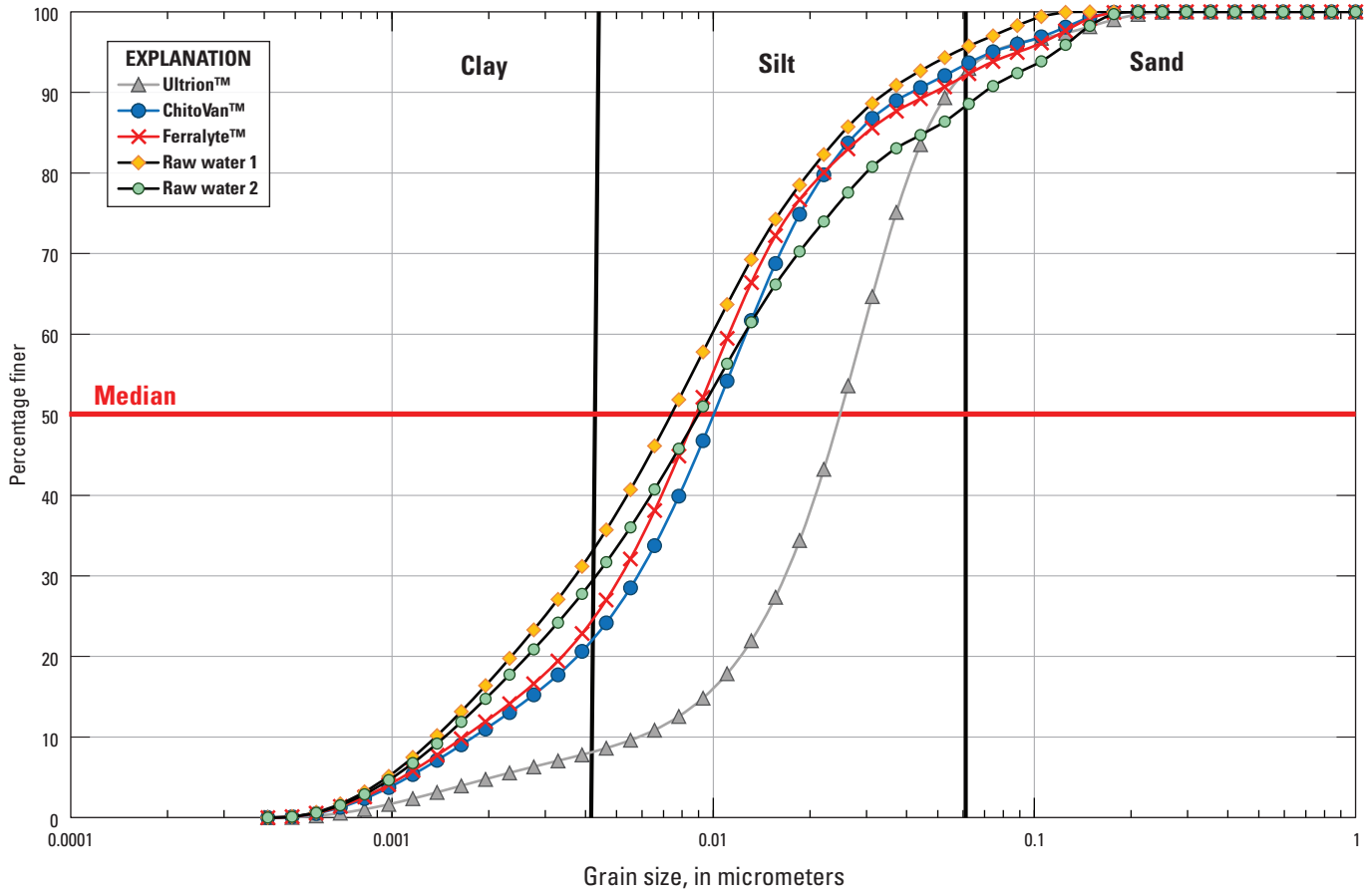

Figure 8. Grain-size distribution curves for the settled materials from the coagulation full experiment and for sediment in non-treated (raw) surface water. The raw water 1 and 2 samples were collected during the coagulation full experiment from the large batch of samples collected on March 17, 2017. Size classifications according to Poppe and others (2000).

Table 5. Summary of grain-size classifications and statistics for settled materials from coagulation treatments and for sediment in non-treated (raw) surface water.

[All grain size distribution analysis performed at the U.S. Geological Survey California Water Science Center Hydrologic Research Laboratory.
Abbreviations: n, number; TM, trademark; µm, micrometer]

Treatment	Sand (percent)	Silt (percent)	Clay (percent)	Average median (µm)	Average 10th percentile (µm)	Average 10th percentile (n)
Ultrion™	5.0	86.3	8.8	20.9	4.9	2
ChitoVan™	5.0	70.3	24.7	8.4	1.5	2
Ferralyte™	6.2	66.2	27.7	7.4	1.4	2
Raw water 1	3.0	61.3	36.0	6.2	1.1	1
Raw water 2	9.2	58.5	32.3	7.6	1.2	1

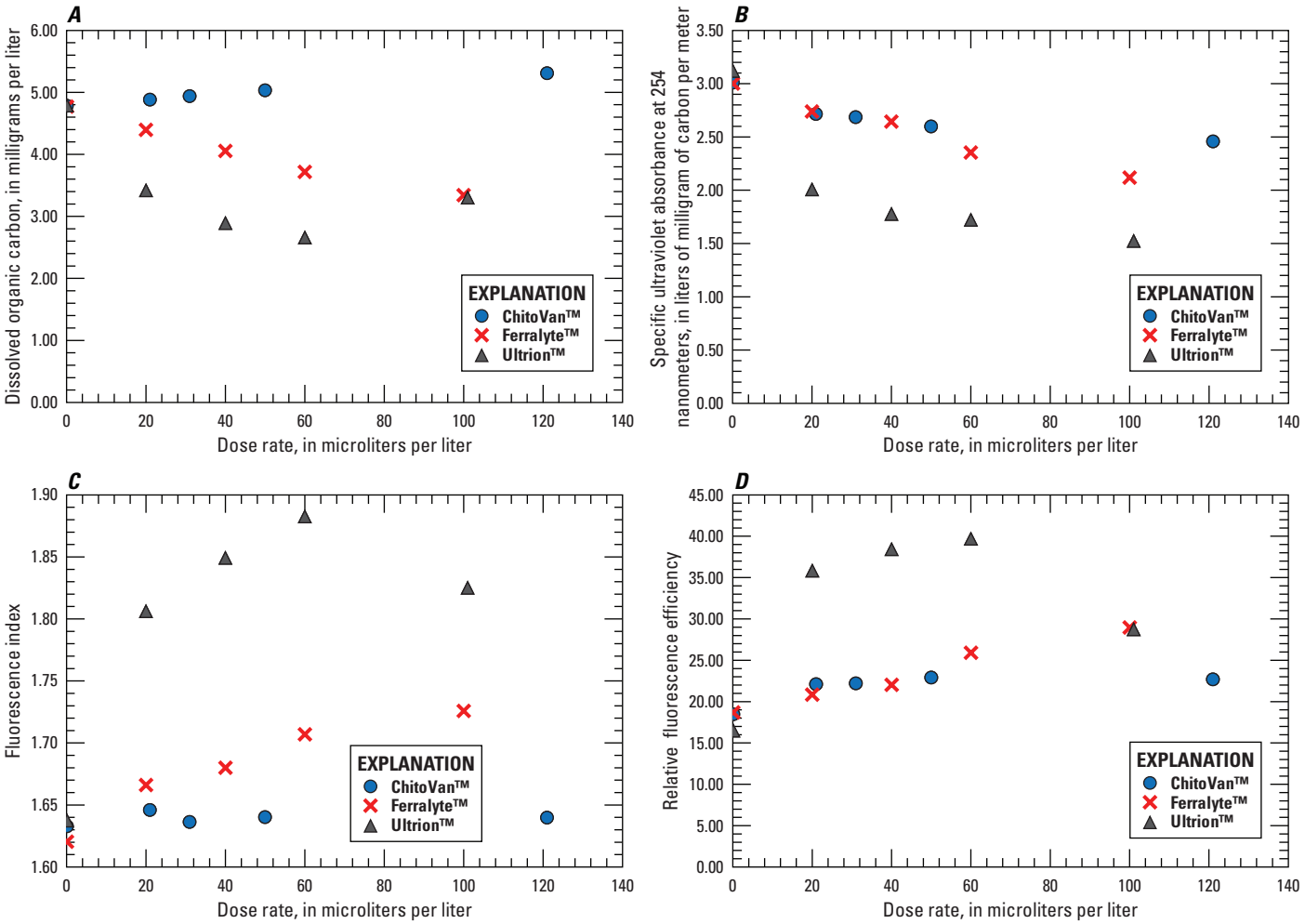

Figure 9. Dose-rate response curves for optical measurements of *A*, dissolved organic carbon; *B*, specific absorbance at 254 nanometers; *C*, fluorescence index; and *D*, relative fluorescence efficiency.

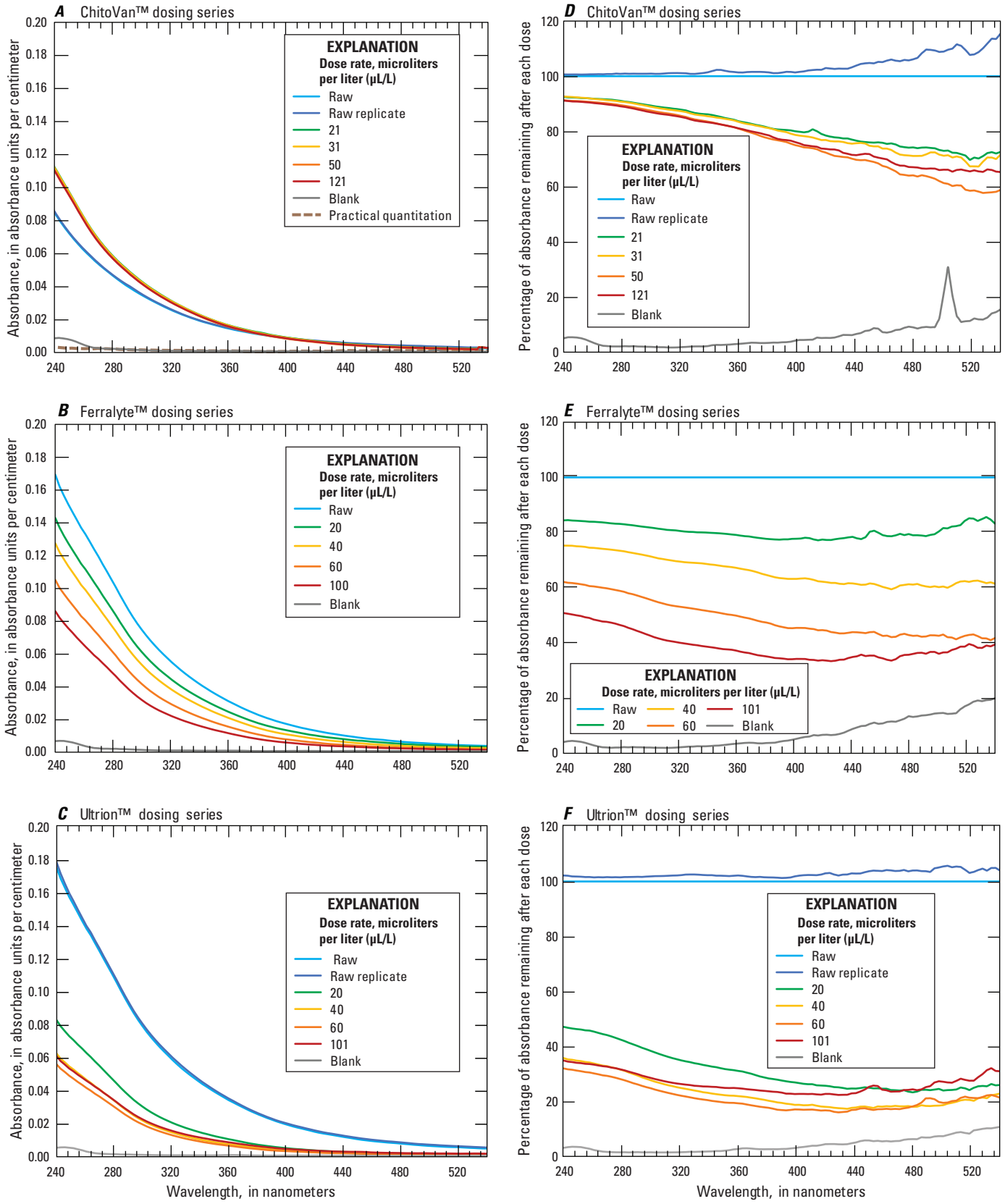

Figure 10. Effect of the coagulants on the ultraviolet absorbance spectra (left-side figures show absorbance measurements for each dose rate; right-side figures show the percent absorbance remaining across the spectra for each coagulant and dose rate). Measurements at wavelengths longer than 540 nanometers were predominantly below the practical quantitative limit and have been omitted.

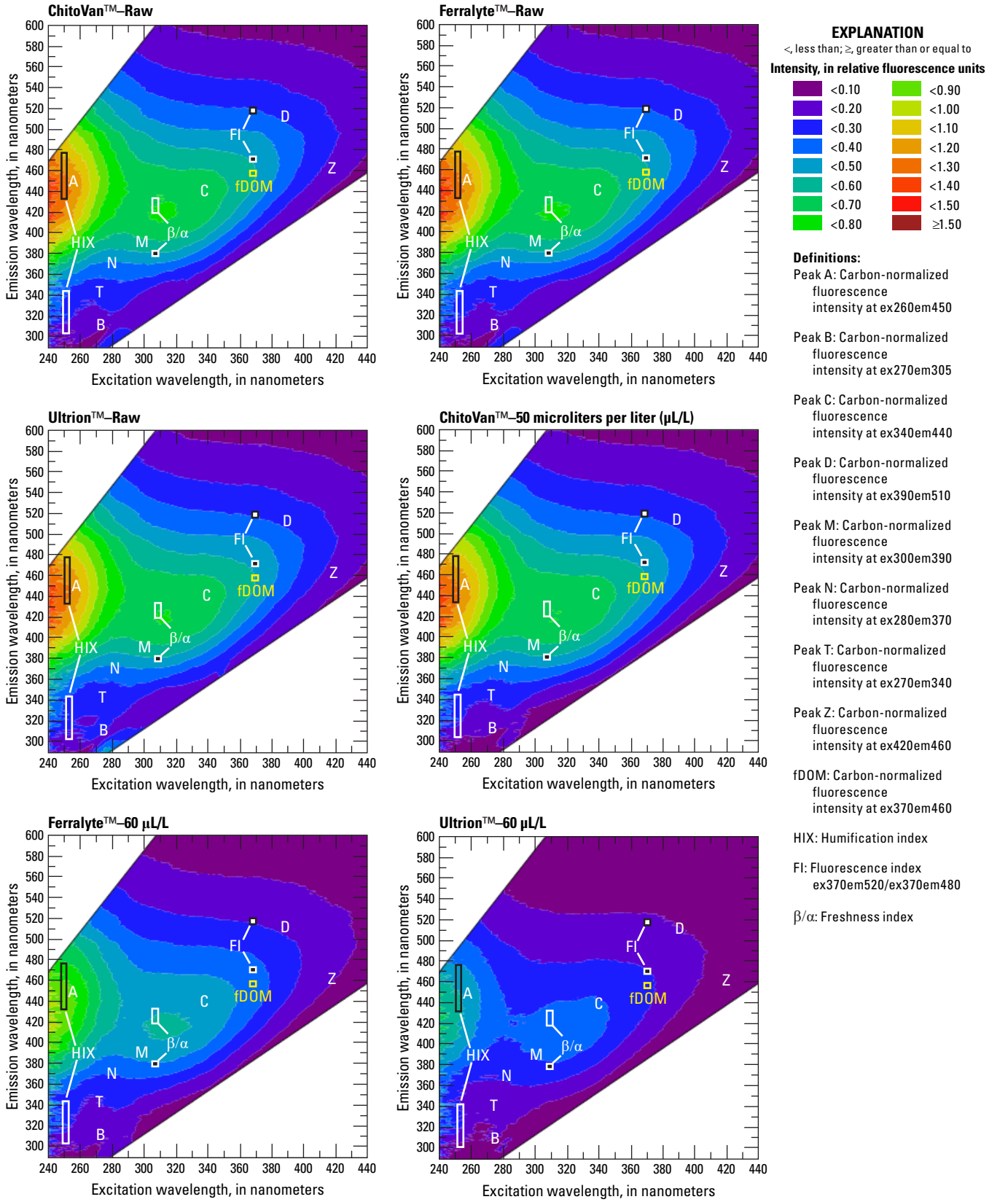

Figure 11. Effects of coagulants on the fluorescence spectra. The first three figures show the excitation emission matrices (EEMs) intensity for the raw-water sample with no coagulant added for each experimental run. The last three figures show the EEMs intensity for the second highest dose rate for each coagulant in the experimental run. Peak intensity is measured in Relative Fluorescence Units (RFU) for all graphs.

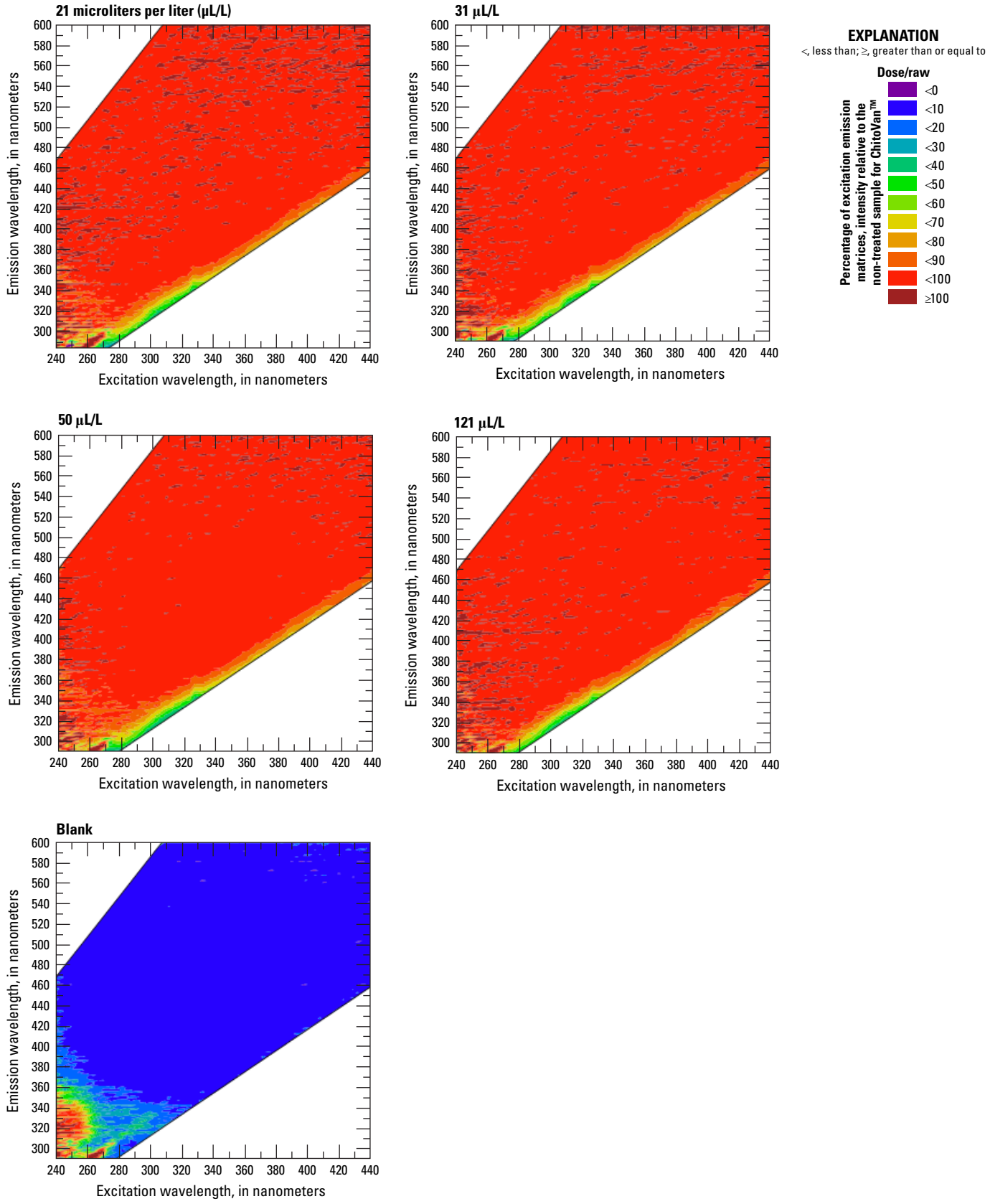

Figure 12. Intensity of excitation emission matrices (EEMs) for samples treated with the ChitoVan™ coagulant, and blank water. Red indicates 100 percent of the initial EEMs intensity, whereas blue indicates less than 10 percent of the initial EEMs intensity remains. The blank shows the EEMs intensity relative to the raw-water sample. Peak intensity is measured in Relative Fluorescence Units (RFU) for all graphs.

In contrast, the addition of Ferralyte™ lowered DOM concentrations and affected optical indicators of DOM character. Ferralyte™ decreased DOC concentrations by 30 percent at the highest dose (fig. 9*A*). The addition of Ferralyte™ decreased total absorbance (fig. 10) and fluorescence (fig. 11) across the measured spectra. The effects of Ferralyte™ dose rates on the optical character were linear over much of the spectral field, indicating that additional dosing would remove additional DOM. However, the loss of fluorescence was in the area of the excitation-emission matrices (EEMs) associated with humic and fulvic acids, whereas the region associated with algal and microbial source (Chen and others, 2003) was unaffected (fig. 13). This preferential removal of humic DOM is consistent with that observed previously (Henneberry and others, 2011).

The addition of Ultrion™ had a response like that of Ferralyte™, but the effect was more pronounced for Ultrion™ at lower dose rates. DOC concentration was decreased by 30 percent at the lowest dose rate, did not change markedly with increasing dose rates, and even increased at the highest dose (fig. 9*A*). Indices of DOC character were most affected by Ultrion™ (figs. 9*B–D*). Most of the decrease in DOC concentration, absorbance, and fluorescence was at the lowest dose rate (20 µL/L), with less additional decreases at higher dose rates. A large loss of absorbance and fluorescence occurred at the lowest dose rate, but the optical signals were enhanced at higher dose rates, increasing to more than 60-percent removal for the highest dose rate for some areas of the measured spectra—even in the algal and microbial region of the spectra (figs. 10, 11, 14). The highest dose rate appeared to release some DOM back into the solution, indicating that overdosing could have a negative effect on coagulant performance.

Other Effects

Other environmentally relevant water-quality characteristics that may be affected by coagulation are specific conductance and pH; these properties are relevant because they affect biogeochemical processes and wildlife health. Few effects of coagulant dosing on the pH or specific conductance were observed. Very little change occurred in pH values for ChitoVan™ between each dose, which ranged from 7.86 to 7.98 (fig. 15*A*). A decrease in pH was caused by the addition of Ferralyte™, which lowered the pH at a rate of 0.21 pH units for each 25-µL/L dose added. This pH response was quite large given the small-dose volumes, indicating that the source samples were poorly buffered for the addition of the iron (II) sulfate-based coagulant. ChitoVan™ caused very little change in specific conductance between each dose rate; conductivity ranged from 367 to 378 microsiemens per centimeter at 25 degrees Celsius (µS/cm at 25 ºC; fig. 15*B*). Similarly for Ferralyte™, no systematic change in specific conductance was observed across the range of dose rates tested, but the conductivity range of 357–387 µS/cm at 25 ºC was wider than for other coagulants.

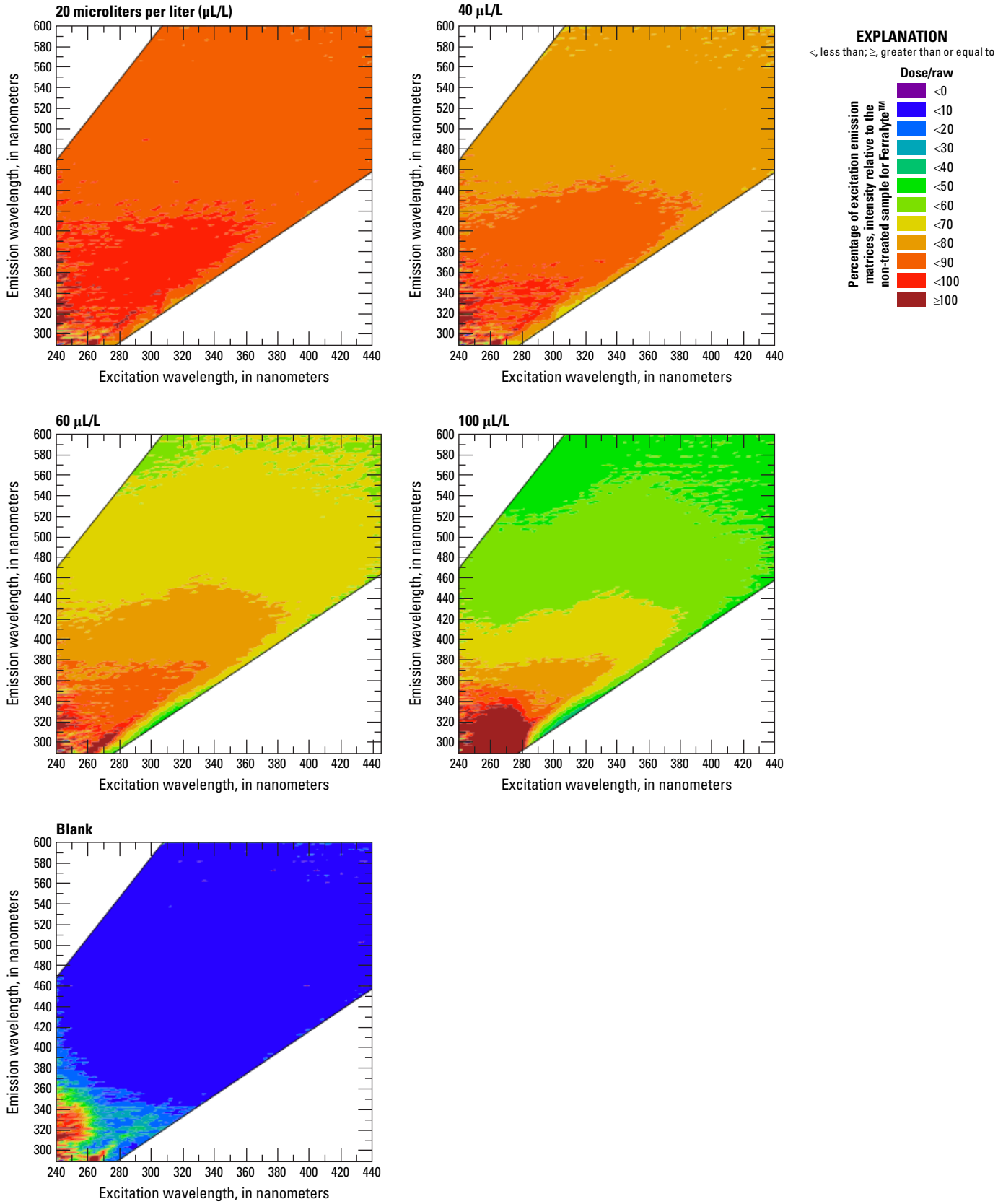

Figure 13. Intensity of excitation emission matrices (EEMs) for samples treated with the Ferralyte™ coagulant and blank water. Red indicates 100 percent of the initial EEMs intensity, whereas blue indicates less than 10 percent of the initial EEMs intensity remains. The blank shows the EEMs intensity relative to the raw-water sample. Peak intensity is measured in Relative Fluorescence Units (RFU) for all graphs.

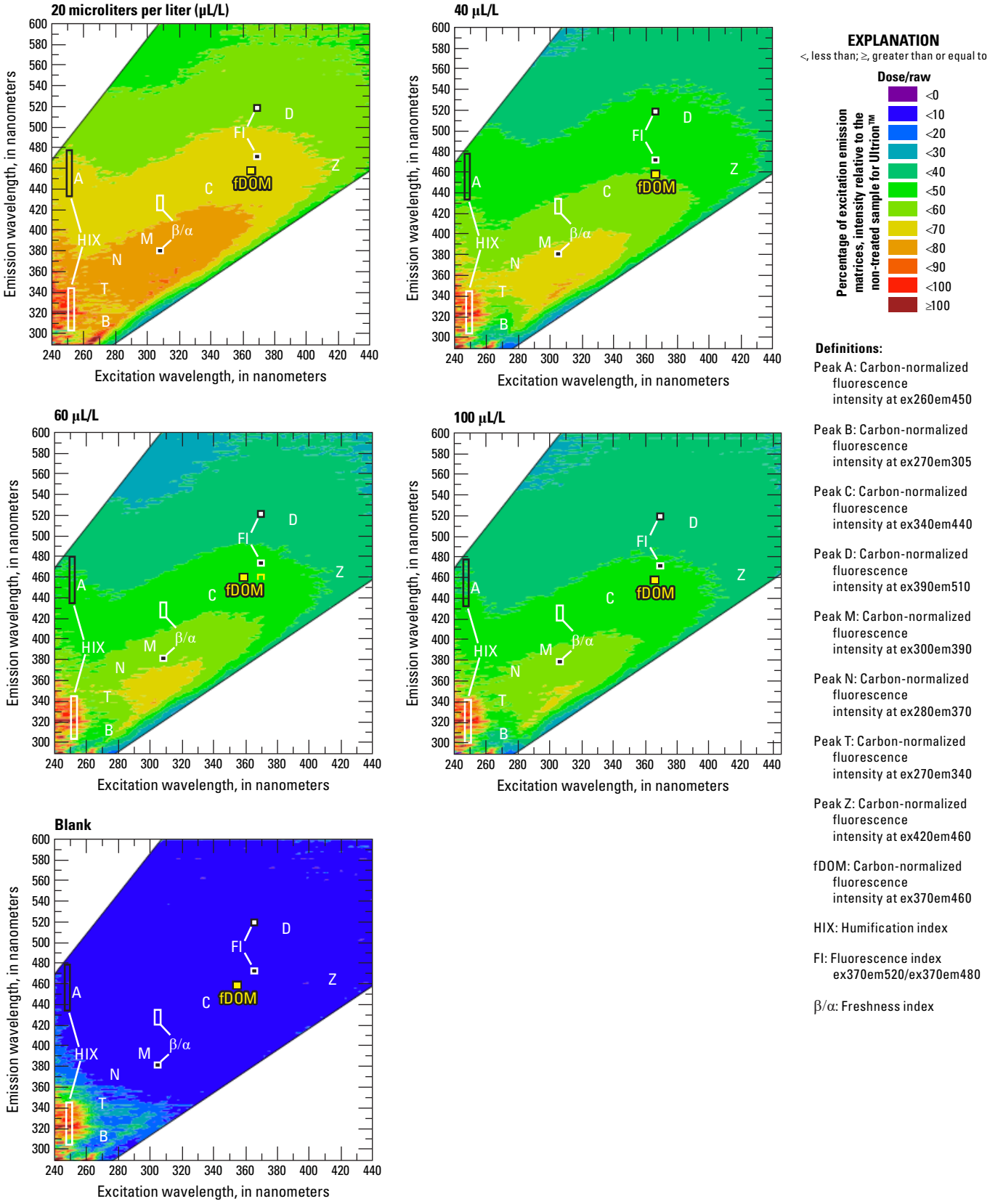

Figure 14. Intensity of excitation emission matrices (EEMs) for samples treated with the Ultrion™ coagulant, and blank water. Red indicates 100 percent of the initial EEMs intensity, whereas blue indicates less than 10 percent of the initial EEMs intensity remains. The blank shows the EEMs intensity relative to the raw-water sample. Peak intensity is measured in Relative Fluorescence Units (RFU) for all graphs.

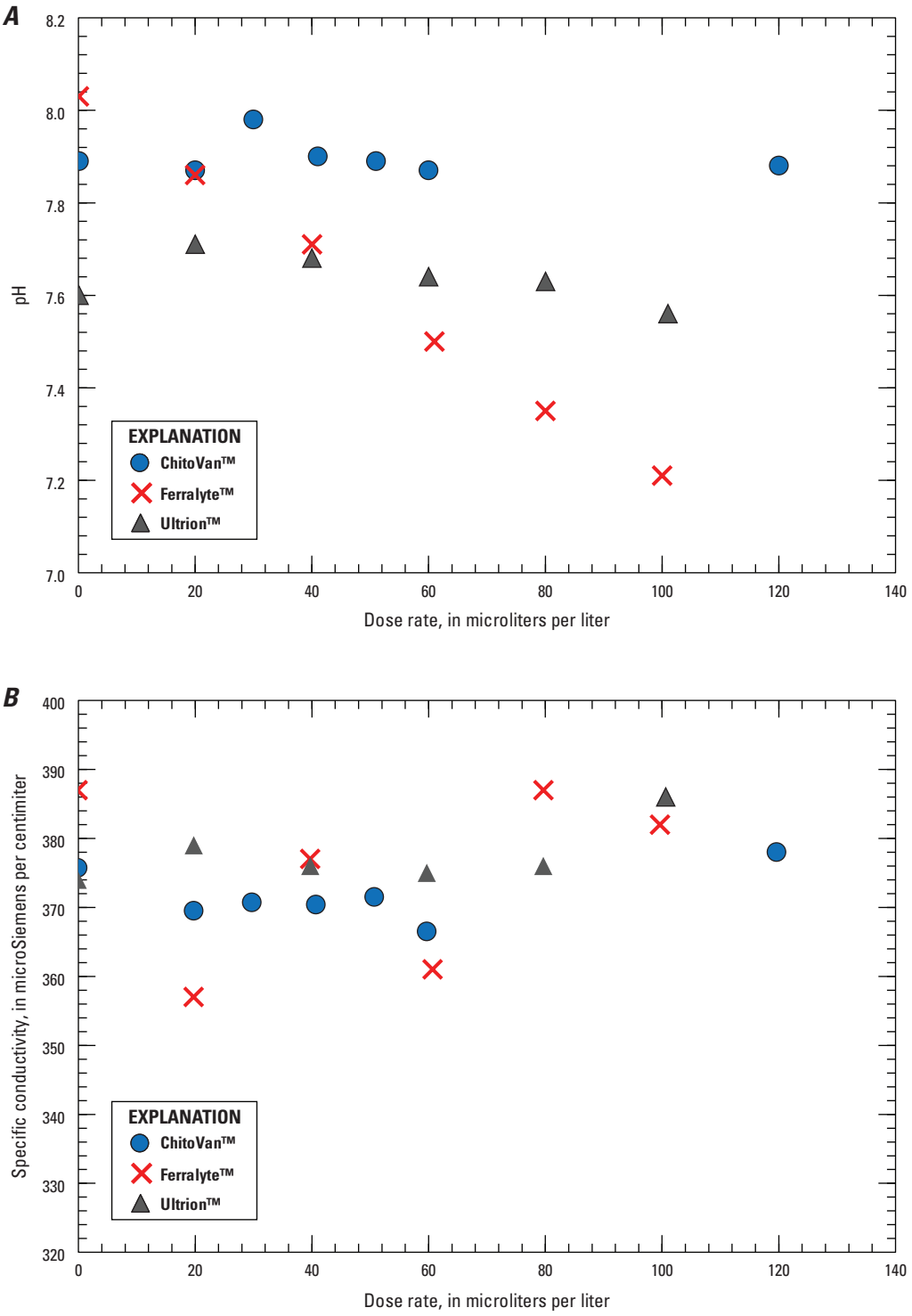

Figure 15. Coagulant dose-rate response curves for *A*, pH and B, specific conductance.

Part 2: Low-Particulate Mercury Samples

The two sample types collected from the Harley Gulch area varied in origin and composition. To effectively evaluate the potential for coagulation and sorbent treatment approaches, the original source-water character of these representative sites was assessed and compared with respect to trace metals and a suite of standard water-quality metrics to provide further context as to the effectiveness of coagulant and sorbent experiments.

Initial Sample Characterization

Water quality of the two low-particulate Harley Gulch source waters (Turkey Creek, 390041122260401; Connate Spring, 390057122262501) used in the sorbent experiments differed markedly. Mercury concentrations, pH, and specific conductance measurements resembled values reported in the literature and for reconnaissance sampling (table 6), indicating consistent concentrations for the water sources. The THg concentrations were similar for the two sources, ranging from 159 to 186 ng/L despite otherwise markedly different chemical characteristics (appendix table 2–1). The specific conductance of the Connate-Spring source was higher in November compared to samples collected in May and values previously reported in the literature. The Turkey Creek samples generally had warmer temperatures, were more enriched in chlorophyll and dissolved oxygen, less enriched in dissolved organic matter, and during the May 2016 experimental run, had higher specific conductance than the connate-spring samples, (approximately 8,400 and 5,000 µS/cm, respectively; table 6). The trace-metal concentrations differed between the source samples; uranium and nickel were higher in the connate-spring samples, whereas sodium and manganese were markedly higher in the Turkey Creek samples (appendix table 6–1).

The characterization of water sources using IOPs revealed the unique signatures of these two sources. There were distinct differences in the absorbance and fluorescence spectra of the water sources (figs. 16, 17). The IOPs for the Turkey Creek and Connate Spring samples revealed by the EEMs indicate a different water chemistry between the two sites. Spectral slopes were markedly higher in the Connate Spring samples than in the Turkey Creek samples, except for wavelengths shorter than 256 nm. The Connate Spring samples had higher overall absorbance, between 245 and 400 nm, than the Turkey Creek samples. Turkey Creek samples had the highest fluorescence intensities in the excitation/emission (ex/em) area of ex240:em390, in a spectral region that has not been well documented and extends out toward the "peak M" region (fig. 17). In contrast, the Connate Spring samples had fluorescence signatures like those of DOM in natural surface waters with the highest intensities in the "peak A" region (fig. 17).

Coagulation Test

Despite evidence of different organic-matter concentrations in samples from the two low-particulate sites (390041122260401; 390057122262501; table 6), the addition of coagulants failed to produce any flocculant material in any samples processed. Dosing with the MetClear™ solution, which is designed to remove metals via co-precipitation, caused a minimal response observed as a slight production of neutrally buoyant white flakes that resulted in a slightly cloudy sample. As a result, the coagulants and the MetClear™ were eliminated from further experimentation with waters from the two low-turbidity sites, and the focus shifted to the use of sorbents to remove dissolved Hg species.

Sorbent Experiments: Methods and Statistics

We constructed a linear fixed-effects model to determine the influence of the experimental variables on the amount of THg removed from the water after passage through the sorbents (appendix tables 4–1, 5–1). "Nanograms (ng) of mercury removed" was the dependent variable (Y) that was calculated as the difference between the THg concentration of the untreated sample (in nanograms per liter) and the concentration of the treated aliquot multiplied by the sample volume (0.5 L). The water sources (390041122260401; 390057122262501), sorbent type (chitosan, coal, or coconut), flow rate (0.1, 0.5, or 1.0 L/min), and total volume passed (0–3 L in increments of 0.5 L) were the fixed effects (x variables). Two-way interactions between flow rate and water source, flow rate and sorbent type, and flow rate and volume passed were included. A single 3-way interaction between water source, sorbent, and flow rate also was included. All statistical analyses were performed using JMP (v12; Cary, North Carolina).

Sorbent-Modeling Results

We observed differences in the removal of THg by sorbent type ($F_{2,31} = 9.77$, F is the F-ratio or statistical test metric that is used when reporting analysis of covariance results; $p = 0.0005$, p is statistical significance), flow rate ($F_{2,31} = 47.6$, $p < 0.0001$), and total volume passed ($F_{1,31} = 13.9$, $p = 0.0008$), but not by water source ($F_{1,31} = 0.422$, $p = 0.5205$; fig. 18; appendix table 4–1). However, there were several significant interactions including source by flow rate ($F_{2,31} = 19.8$, $p < 0.0001$), source by sorbent type ($F_{2,31} = 4.464$, $p = 0.0198$), and the 3-way interaction of source by sorbent by flow rate ($F_{4,31} = 6.33$, $p = 0.0008$), indicating that the effects of the variables on the THg removal from these waters are complicated and require a reduction in the total number of model variables for better interpretation of individual variable effects.

Table 6. Field surface-water-quality measurements for sampling sites in the Harley Gulch area collected in November 2015 and May 2016.

[C, creek; fDOM, fluorescent dissolved organic matter; FNU, Formazin Nephelometric Unit; ID, identification; hh:mm, hour:minute; mg/L, milligrams per liter; mm/dd/yyyy, month/day/year; mm Hg, millimeters of mercury; nr, near; PDT, Pacific Daylight Time; QSU, quinine sulfate unit; Trib, tributary; USGS, U.S. Geological Survey; —, no data exists; [], USGS parameter code; °C, degrees Celsius; µg/L, micrograms per liter;
µS/cm, microsiemens per centimeter]

Field ID	USGS station ID	Date (mm/dd/yyyy)	Time (PDT) (hh:mm)	Temperature (°C) [00010]	Specific conductivity (µS/cm) [00095]	Dissolved oxygen (mg/L) [00300]	Dissolved oxygen (percent) [00301]	Barometric pressure (mmHg) [00025]	pH [00400]	Turbidity (FNU) [63680]	fDOM (QSU) [32295]	Chlorophyll (µg/L) [32316]
Connate Spring A Unnamed Trib nr Wilbur Springs CA	390041122260401	11/16/2015	12:30	14.8	6,820	9.34	94.5	725.9	8.01	1.2	195.4	6
Connate Spring A Unnamed Trib nr Wilbur Springs CA	390041122260401	05/03/2016	11:40	14.2	5,041	9.05	89	719.6	8.16	0.5	218	5.8
Connate Spring A Unnamed Trib nr Wilbur Springs CA	390041122260401	05/04/2016	15:30	14.2	5,078	8.85	87.6	714.8	8.16	0.4	219.9	6.7
Connate Spring A Unnamed Trib nr Wilbur Springs CA	390041122260401	05/04/2016	17:30	14.2	5,050	9.07	—	714.7	8.18	0.4	220	5.7
Connate Spring A Unnamed Trib nr Wilbur Springs CA	390041122260401	05/05/2016	12:30	13.9	5,046	8.98	88.4	715.6	8.2	0.5	218	6.2
Turkey C nr Wilbur Springs CA	390057122262501	11/16/2015	14:30	15.5	8,250	9.7	100	723.2	8.37	3	70.8	20
Turkey C nr Wilbur Springs CA	390057122262501	05/03/2016	10:30	23.3	8,412	9.7	117	717.4	8.4	1	89.5	30
Turkey C nr Wilbur Springs CA	390057122262501	05/04/2016	9:10	20.1	8,379	7.99	90.6	713.8	8.36	1	84.3	29.7
Turkey C nr Wilbur Springs CA	390057122262501	05/04/2016	11:40	23.6	8,404	10.49	127.1	714	8.41	0.9	88.4	30
Turkey C nr Wilbur Springs CA	390057122262501	05/04/2016	13:40	26.8	8,433	11.4	147.1	713.1	8.42	1.2	93.2	21.8
Turkey C nr Wilbur Springs CA	390057122262501	05/05/2016	9:40	18.6	8,390	7.75	85.2	713.4	8.38	1	81	32

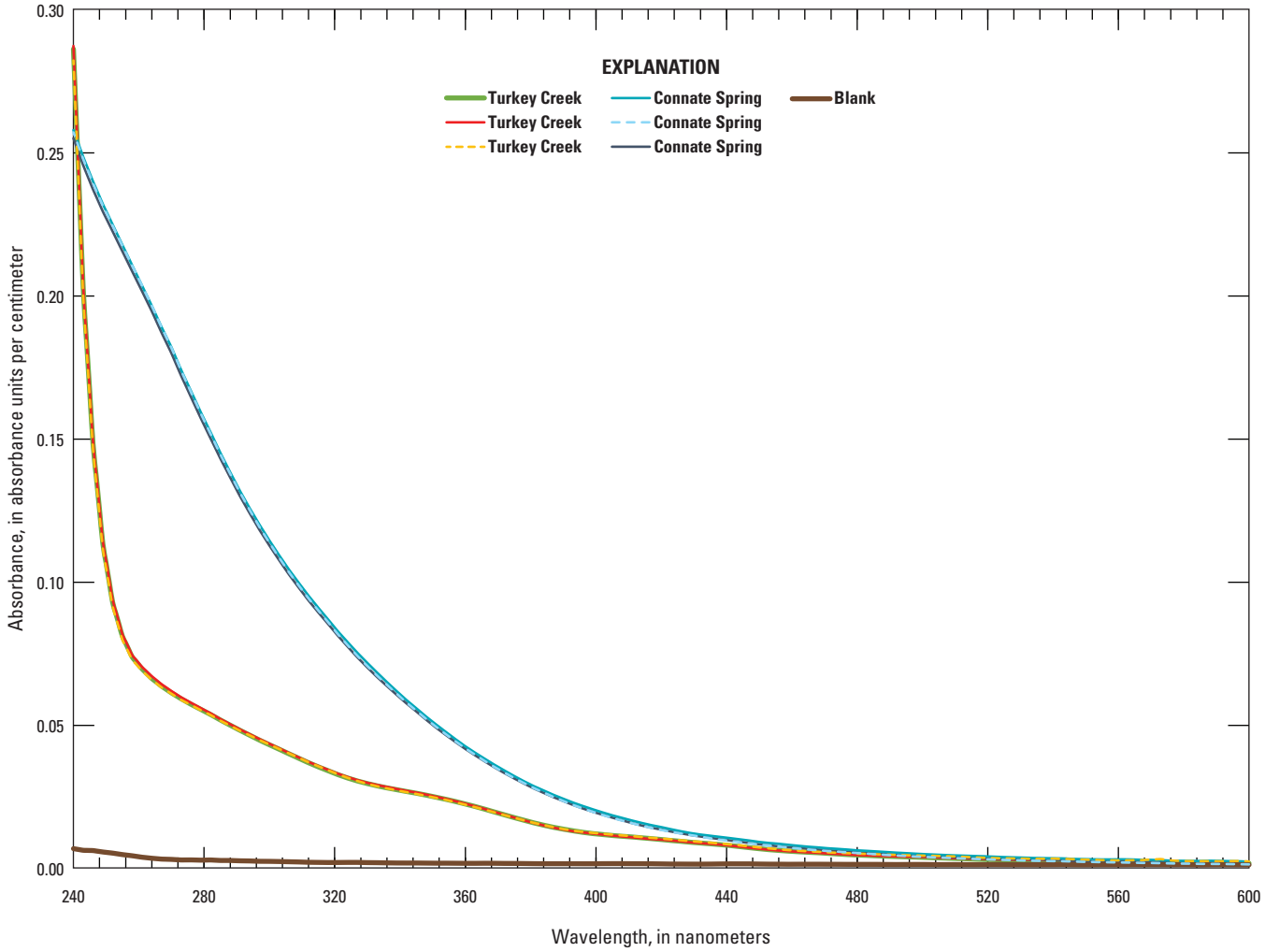

Figure 16. Absorbance spectra for the low-particulate source waters. Three samples were collected from each site between May 4 and 5, 2016. The results for blank water are provided for reference.

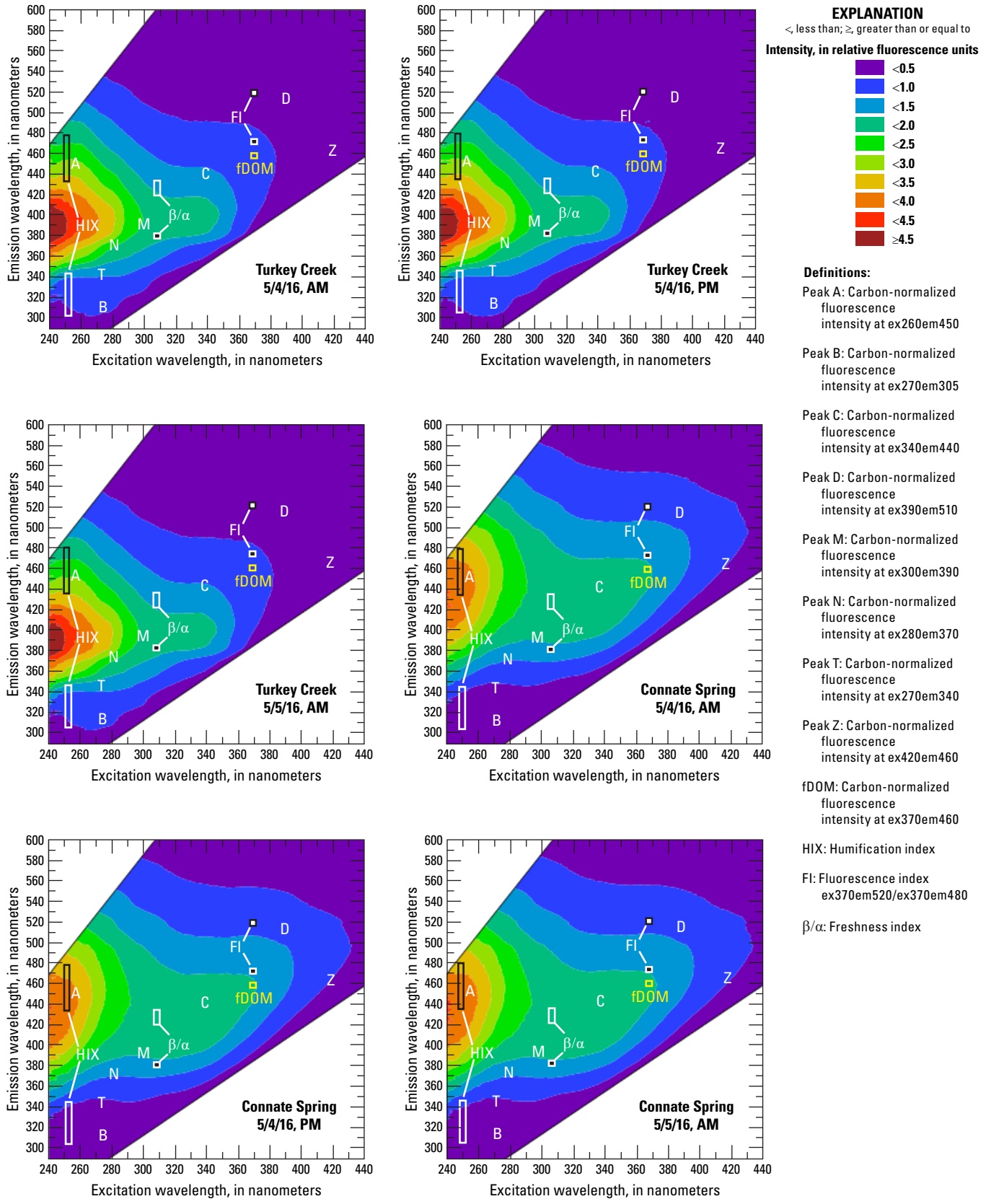

Figure 17. Excitation-emission matrix (EEM) plots showing the differences in fluorescence spectra of the three samples from each of the two source waters used in the sorbent experiment May 4–5, 2016. The fluorescent signature of each water source was consistent across sample collections. Peak intensity is measured in percent Relative Fluorescence Units (RFU) for all graphs.

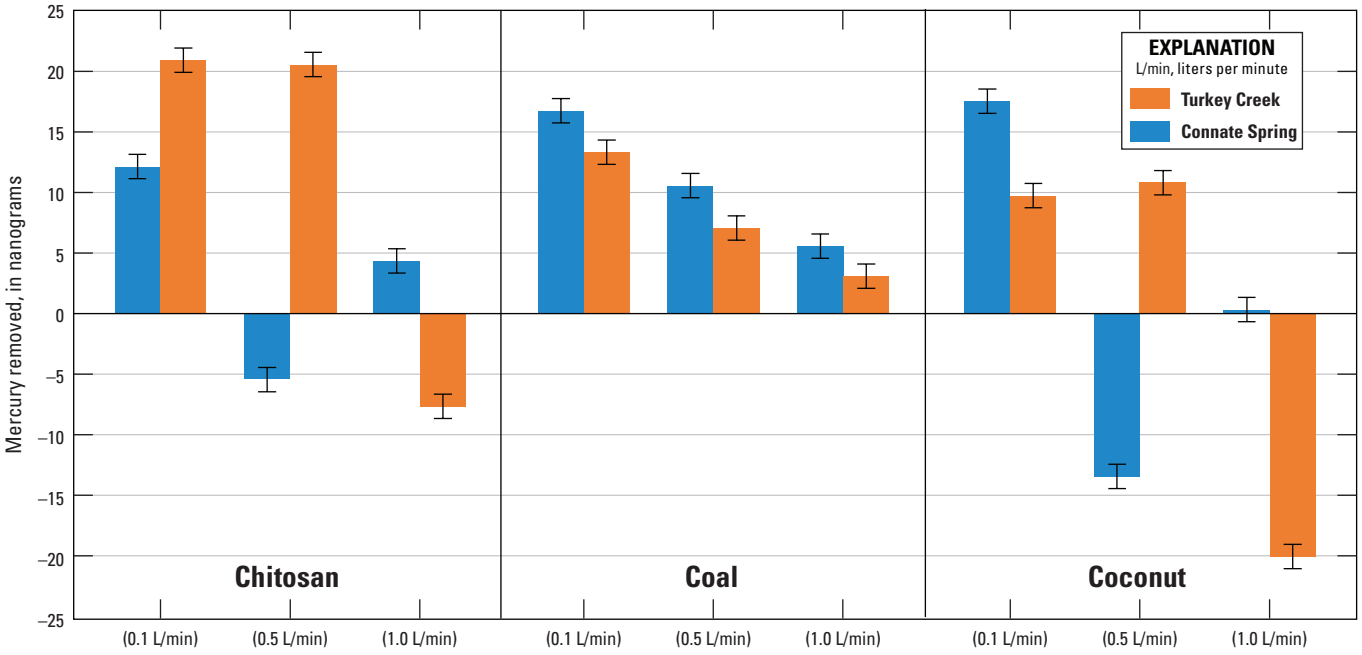

Figure 18. Least squares mean (plus or minus standard error) for total mercury (THg) removed using a linear fixed effects model including water source, sorbent type, and flow rate as fixed effects ($r2 = 0.86$; $p < 0.0001$).

We focused further evaluation on the flow rate where we had the greatest response and the greatest number of observations, the 0.1-L/min flow rate (appendix table 5–1). The coal sorbent is the most versatile of the sorbents, effectively removing THg from both water sources and showing only a small decrease in the THg removal rate as the total-volume passed increased (figs. 18, 19). In contrast, the effectiveness of the coconut sorbent appears to decrease relatively quickly compared to that of the other sorbents tested, perhaps indicating a lower binding capacity for Hg(II). The chitosan sorbent was more effective at removing THg from the Turkey Creek sample compared to the Connate-Spring sample, but its effectiveness was not decreased markedly as more water passed, indicating that it may be more of a kinetic effect than an inhibition of binding.

Dissolved trace-metal concentrations did not change markedly after the water passed through any of the tested sorbents (appendix table 6–1). Trace-metal concentrations in treated water samples were in the same ranges as those in the non-treated water samples. Blank samples had trace-metal concentrations that were variable for the concentration ranges measured in the samples, limiting the ability to observe any trends.

Discussion

Active- and passive-treatment approaches to control the mobilization of Hg may prove feasible with widely available technologies and materials. The use of coagulants to sequester MeHg and THg from surface water was highly effective in laboratory experiments, removing as much as 90 percent of the THg in suspension with the addition of only one unit of the Ultrion™ coagulant (1.5-percent solution) per 50,000 units of source water (1:50,000 ratio). Ultrion™ also is available as a 3-percent solution, meaning dose rates could readily be halved with products currently on the market. The other coagulants also removed substantial amounts of the MeHg and THg in suspension at dose ratios of 1:10,000–1:30,000, but the Ultrion™ coagulant was the only one that lowered the MeHg concentration to less than the Sacramento–San Joaquin Delta MeHg TMDL implementation goal of 0.06 ng/L (Wood and others, 2010). Ultrion™ also produced the largest and most physically stable aggregates. Ultrion™ may have performed better because it was used on the remaining high-particulate samples, had been refrigerated for 11 days after the collection date, and natural coagulation may have occurred.

Dose ratios of this scale make large-scale applications a realistic possibility for management challenges such as that of the CCSB where stormflows that carry large quantities of MeHg and THg downstream to sensitive habitats can reach into the millions of liters per minute (Cooke and others, 2004; C.N. Alpers, U.S. Geological Survey, oral commun., 2017). Coagulation-based systems are typically applied to flow rates of a few to dozens of cubic meters per second. Addressing the scale of these treatment systems is essential to the feasibility of future implementation at a site such as the CCSB. For instance, applying a dose rate of 20 µL/L of water at a daily average flow of 57 m^3/s requires approximately 100,000 L of coagulant per day. Although challenging, a passive system employing a silo-fed coagulant storage and delivery system could operate unattended for a week before needing to be refilled.

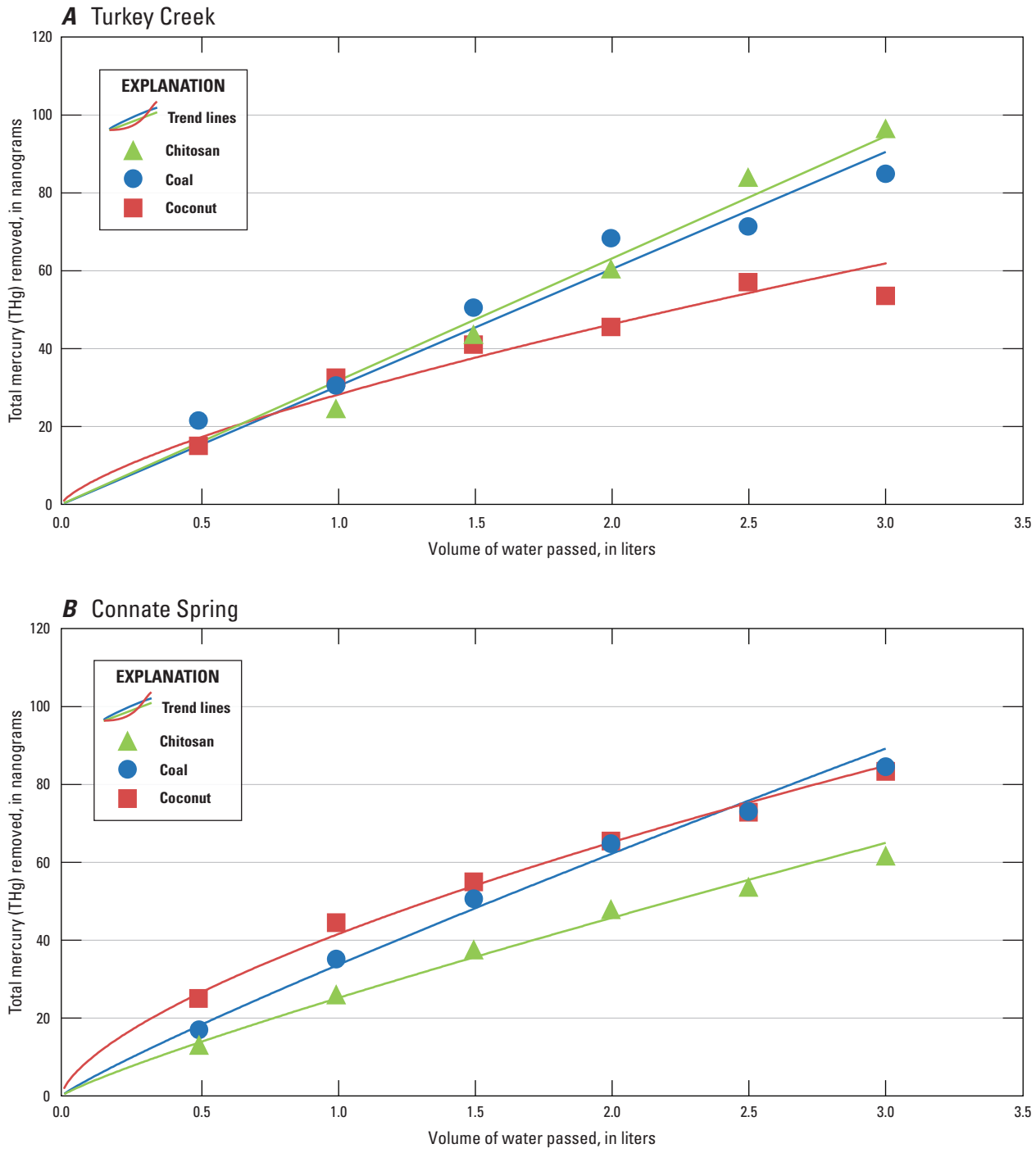

Figure 19. Amount of total mercury (THg) removed from surface water passing through sorbents tested at the 0.1-liter per minute (L/min) flow rate for the *A,* Connate Spring and *B,* Turkey Creek.

Although it may not be feasible to fully treat the entire volume of water entering the CCSB throughout the winter, targeted approaches could substantially lower the amount of MeHg and THg transported downstream to the Sacramento–San Joaquin Delta and San Francisco Bay. For instance, an approach that targets treatment of only the highest flows that carry the greatest amounts of Hg could be achieved for a short period of time. In systems like the CCSB, a single large storm can transport most of the MeHg and THg loads for the entire winter (C.N. Alpers, U.S. Geological Survey, oral commun., 2017). Alternatively, a more traditional scaled-dosing system (less than 12,000 L/min) could treat portions of the stormflows in a subbasin, thus avoiding the challenges associated with excessively high dosing rates and supply requirements for large storm peaks in these watersheds. Although outside of the scope of this project, a full economic analysis is warranted to evaluate this technically feasible approach, especially when comparing this approach to landscape-scale alternatives employed to control Hg and MeHg transport (Randall and Chattopadhyay, 2013).

Although promising, the use of coagulants to reduce MeHg and THg in surface water, especially in a passive-dosing approach that allows the resulting flocculants to settle in the natural environment, will require further assessments with respect to their stability and potential for toxicity to plants and wildlife. ChitoVan™ is the only coagulant that has been reported to be non-toxic in the environment and has been used to enhance plant growth (Freepons, 1997). However, fish and wildlife have survived in previous field-based studies using metal salt-based in-situ coagulation systems (Stumpner and others, 2015; Liang, 2016), and one previous study even showed lower Hg bioaccumulation in fish inhabiting wetlands receiving salt-based coagulant doses (Ackerman and others, 2015). The use of Ferralyte™ would add more sulfate to the system, potentially stimulating methylation. However, the addition of iron has been shown to impede methylation in laboratory- and field-based mesocosm studies (Mehrotra and others, 2003; Ulrich and Sedlak, 2010). Despite these positive anecdotes, to our knowledge, no formal testing of metal salt-based coagulants on biotic diversity and ecosystem health has been performed.

The mechanisms by which MeHg and THg are removed via coagulation indicate that any adverse effects from the Hg accumulated in sediments are unlikely, although further study is necessary to confirm effects. In the case of particulate-dominated Hg transport, the coagulant serves merely as a bridge or charge neutralizer that promotes the aggregation of fine particles into larger and denser particles that settle more quickly (Ghernaout and Ghernaout, 2012). These aggregates also can physically sequester Hg from interacting with biological processes by creating large particles, thus effectively lowering the Hg potential for further transformation and bioaccumulation. Enhanced nucleation and aggregation of colloids also would effectively lower bioavailability of Hg(II) to methylating bacteria (Graham and others, 2012; Hsu-Kim and others, 2013). The decrease in specific ultraviolet absorbance at 254 nanometers ($SUVA_{254}$) associated with coagulant addition is consistent with a preferential removal of large molecular-weight, aromatic-DOM structures (Henneberry and others, 2011). This hypothesis is further supported by fluorescence indicators of dissolved organic matter character (fluorescence index; relative fluorescence efficiency) measured in this study (fig. 9).

Sorbents proved to be less effective than coagulation under the experimental conditions tested, with more effective THg removal at the 0.1-L/min flow rate (10-second contact) than at other rates (appendix table 2–1). The chitosan sorbent was the most effective at removing THg from the Turkey Creek source water. The amounts of THg removed at the 0.1- and 0.5-L/min flow rates (10- and 2-second contact times, respectively) were nearly identical, indicating that chitosan can handle a higher flow rate than other sorbents. At high flow rates, the chitosan and coconut sorbents showed an increase in THg concentrations (fig. 18), which could be attributed to "stripping" of Hg from the sorbent materials that was present originally, or not enough contact time between the sorbents and the sample water. The conditions of the sorbent experiments were established with affordability and feasibility in mind. The sorbent materials used in this study were not modified in any way, and the flake form of chitosan used was fairly effective at the lowest flow rate. More effective Hg removal could potentially be achieved through two scenarios: (1) using the same materials used in this study but increasing the size of the sorbent system or (2) enhancing the sorbent materials used. An increase in the size of the trapping system could increase Hg removal. This size increase could come with additional costs. However, the amount of sorbent needed to achieve more Hg removal may not be feasible to maintain over a long period of time. Longevity or capacity of the sorbents was not tested.

Increased Hg removal could be achieved by enhancement of the sorbent materials. Modified chitosan and its derivatives have been extensively studied as materials to aid in heavy-metal removal because of their relatively low cost and high availability (Miretzky and Cirelli, 2009; Lui and Bai, 2014). Chitosan beads linked with organic compounds were reported to be effective in removing copper from solution (Osifo and others, 2009). Chitosan coalesced with activated carbon also have shown promising results in removing dyes from wastewater (Auta and Hameed, 2013). There have been recent advances in using other materials as potential sorbents. One study by Chavan and others (2016) used coffee grounds combined with silicone polymers to create a foam to trap heavy metals from wastewater. The foams were reported to be effective at removing lead and Hg, and the foam structure made for easy handling and disposal. Gilmour and others (2013) demonstrated that adding activated carbon to sediments contaminated with Hg reduced bioaccumulation in local organisms in the sediment, which indicates a promising method for addressing Hg-contaminated soils. Studies using different materials to remove Hg from aqueous solutions have been ongoing for years. Knocke and Hemphill (1981) showed that ground vulcanized rubber was effective at removing Hg from solutions.

During low-flow conditions typically seen in the summer in the Sacramento Valley, the use of sorbents would be a feasible approach to removing dissolved Hg from waters entering sensitive habitats like wetlands. During high-flow storm conditions in the Cache Creek watershed, however, sorbents would be overwhelmed by particulate-rich water and would be unable to accommodate removal of dissolved or colloidal Hg during high-flow rates. Under such conditions, the focus could shift to particulate removal with coagulants. Targeted approaches of coagulant dosing in the Cache Creek watershed could substantially decrease the amount of Hg entering the Sacramento–San Joaquin Delta.

Summary

Coagulants and sorbents were investigated by the U.S. Geological Survey, in cooperation with the U.S. Environmental Protection Agency, as a means of immobilizing and removing mercury (Hg) from water collected from sites with high levels of Hg in the Cache Creek watershed. The Cache Creek watershed, in the northern California inner Coast Ranges, provides a model watershed for studying the control of Hg contamination and mobilization in a catchment with extensive areas of sensitive habitats downstream. The high levels of Hg in the watershed sediment are from natural background geologic sources that could have been exacerbated by mining activities.

Both particulate-dominant and dissolved-dominant Hg source waters were selected for sampling and laboratory experimentation. The high-particulate samples were collected in March 2016 from the Cache Creek Settling Basin (CCSB), whereas the low-particulate Hg samples were collected May 3, 2016, from two locations in the Harley Gulch area. One site in the Harley Gulch area is approximately 100 meters (m) downstream from a geothermal spring, and the second site is at the emergence point of a connate-water spring. The low-particulate samples selected for sorbent testing were chosen because of high, naturally present Hg levels and a replenishing source that could potentially allow for a field setting for testing of the sorbents. The particulate-dominant sample was treated with varying doses of three coagulants— (1) ChitoVan™ HV 1.5 percent (shell based), (2) Ferralyte™ 8131 (ferric sulfate based), and (3) Ultrion™ 8186 (aluminum based)—then mixed on a stir plate and allowed to settle for 40 minutes. The low-particulate Hg sample was passed through exchange columns packed with three different sorbents— (1) solid-phase chitosan flakes, (2) charred coconut husks, and (3) coal pellets. For the particulate-dominant source, samples of a settled flocculant were collected during a "clean" experimental run in which Hg clean techniques were enforced. For the low-particulate Hg samples, water was passed through the packed exchange columns at three different flow rates (1.0, 0.5, and 0.1 liter per minute), representing realistic contact times for passive exchange bed applications (1–10 seconds, respectively), and then collected into bottles for Hg analysis.

Coagulation was effective at removing particulate Hg (table 7). At the lowest dose amounts, ChitoVan™ achieved a 59- to 61-percent decrease in methylmercury (MeHg) concentrations and a 71- to 75-percent decrease in total mercury (THg) concentrations. Ferralyte™ achieved a 37- to 48-percent decrease in MeHg concentrations and a 37- to 48-percent decrease in THg concentrations. Ultrion™ achieved a greater than 90-percent decrease in MeHg and THg concentrations at the lowest dose (20 µL).

The use of sorbents was effective at removing Hg from the filter-passing phase, but sorbents were less effective than coagulation for the flow rates and water:sorbent ratios tested (table 7). Less than 30 percent of the filter-passed THg was removed, even at the lowest flow rate (10-second contact time). Coal-based activated carbon appears to be the most versatile of the three sorbent materials, but overall filter-passing THg removal was less effective than expected. Conditions of the experiment were established with simple design, logistical feasibility, and affordability in mind, and more effective removal of Hg may be achieved through increasing the amount of sorbent per unit of source water and increasing contact time. Further research is needed to determine the sorption capacity and stability of the sorbents.

Table 7. Summary of results from the coagulant and sorbent experiment.

[Percent removal is shown for the lowest dose amounts of each coagulant. Turbidity measurements were collected from the Hach turbidometer and represent turbidity values for all dose amounts. **Abbreviations**: TM, trademark; >, greater than; %, percent]

Coagulants selected	Methyl-mercury reduction (percent)	Total mercury reduction (percent)	Turbidity reduction (percent)
ChitoVan™ HV 1.5%	59–61	71–75	85–91
Ferralyte™ 8131	37–48	37–48	54–93
Ultrion™ 8186	>90	>90	99
Sorbents selected	**Efficiency of mercury removal**		
Chitosan (shell-based)	More effective at removing mercury from Turkey Creek than Connate Spring, removed the highest amount of mercury overall for the Turkey Creek source sample.		
Coconut-based activated carbon	Quick decrease in the effectiveness of mercury removal for both source waters, removed the highest amount of mercury overall for the Connate Spring source water.		
Coal-based activated carbon	Most versatile, removed mercury at all three flow rates, but did not achieve the highest amounts of removal overall.		

Our results compare well with those of Henneberry and others (2011) and Stumpner and others (2015) where the effectiveness of using coagulants to lower MeHg and THg was demonstrated in experimental wetlands. The use of coagulants to sequester MeHg and THg from surface water was highly effective in these laboratory experiments, removing as much as 90 percent of the THg in suspension with the addition of only one unit of Ultrion™ coagulant per 50,000 units of source water (1:50,000 ratio). Dose ratios of this scale make large-scale applications a realistic possibility for management challenges such as that of the CCSB where stormflows that carry large quantities of MeHg and THg downstream to sensitive habitats can reach millions of liters per minute. Although it may not be feasible to fully treat the entire volume of water entering the CCSB throughout winter storms, targeted approaches could substantially lower the amount of Hg transported downstream to the San Francisco Bay and Sacramento–San Joaquin Delta.

References Cited

Ackerman, J.T., Kraus, T.E.C., Fleck, J.A., Krabbenhoft, D.P., Horwath, W.E., Bachand, S.M., Herzog, M.P., Hartman, C.A., and Bachand, P.A.M., 2015, Experimental dosing of wetlands with coagulants removes mercury from surface water and decreases mercury bioaccumulation in fish: Environmental Science and Technology, v. 49, no. 10, p. 6304–6311, https://doi.org/10.1021/acs.est.5b00655.

Alpers, C.N., Yee, J.L., Ackerman, J.T., Orlando, J.L., Slotton, D.G., and Marcin-DiPasquale, M., 2016, Prediction of fish and sediment mercury in streams using landscape variables and historical mining: Science of the Total Environment, v. 571, p. 364–376, https://ac.els-cdn.com/S004896971631018X/1-s2.0-S004896971631018X-main.pdf?_tid=141a4a2a-d9a8-4fc8950c522ce4097d2f&acdnat=1530904372_ae4b14358c21bd552f542ab3c76a1ce8.

Auta, M., and Hameed, B.H., 2013, Coalesced chitosan activated carbon composite for batch and fixed-bed adsorption of cationic and anionic dyes: Colloids and Surface B: Biointerfaces, v. 105, p. 199–206, https://www.sciencedirect.com/science/article/pii/S0927776512007163?via%3Dihub.

Beckman Coulter Inc., 2011, LS 13 320 Laser diffraction particle size analyzer, instruction for use: Brea, Calif., Beckman Coulter, Inc., accessed March, 14, 2017, at https://www.beckmancoulter.com/wsrportal/techdocs?docname=B05577AB.pdf.

Benoit, J.M., Mason, R.P., Gilmour, C.C., and Aiken, G.R., 2001, Constants for mercury binding by dissolved organic matter isolates from the Florida Everglades: Geochimica et Cosmochimica Acta, v. 65, p. 4445–4451, https://repository.si.edu/bitstream/handle/10088/2855/Benoit_et_al_GCA_2001.pdf.

Bratby, J., 2006, Coagulation and flocculation in water and wastewater treatment (2d ed.): London, United Kingdom, IWA Publishing, https://www.iwapublishing.com/news/coagulation-and-flocculation-water-and-wastewater-treatment.

Chavan, A.A., Pinto, J., Liakos, I., Bayer, I.S., Laucielo, S., Athanassiou, A., and Fragouli, D., 2016, Spent coffee bioelastomeric composite foams for the removal of Pb^{2+} and Hg^{2+} from water: ACS Sustainable Chemistry Engineering, v. 4, p. 5495–5502, https://pubs.acs.org/doi/abs/10.1021/acssuschemeng.6b01098.

Chen, W., Westerhoff, P., Leenheer, J.A., and Booksh, K., 2003, Fluorescence excitation— Emission matrix regional integration to quantify spectra for dissolved organic matter: Environmental Science and Technology, v. 37, p. 5701–5710, https://pubs.acs.org/doi/pdf/10.1021/es034354c.

Churchill, R., and Clinkenbeard, J., 2003, Task 5C1: Assessment of the feasibility of remediation of mercury mine sources in the Cache Creek Watershed: CALFED Bay-Delta Mercury Project, 58 p., accessed June 23, 2015, at http://loer.tamug.edu/calfed/Report/Final/Calfed_Mercury_Final_Report_Task5C1_091503.pdf.

Cooke, J., Foe, C., Stanish, S., and Morris, P., 2004, Cache Creek, Bear Creek, and Harley Gulch TMDL for mercury, Staff Report: Rancho Cordova, Calif., Central Valley Regional Water Quality Control Board, 120 p., https://www.waterboards.ca.gov/centralvalley/water_issues/tmdl/central_valley_projects/cache_sulphur_creek/cache_nov2004_a.pdf.

DeWild, J.F., Olson, M.L., and Olund, S.D., 2002, Determination of methyl mercury by aqueous phase ethylation, followed by gas chromatographic separation with cold vapor atomic fluorescence detection: U.S. Geological Survey Open-File Report 01–445, 14 p., accessed July 25, 2016, at https://pubs.usgs.gov/of/2001/ofr-01-445/.

Domagalski, J.L., Slotton, D.G., Alpers, C.N., Suchanek, T.H., Churchill, R., Bloom, N., Ayers, S.M., and Clinkenbeard, J., 2003, Summary and synthesis of mercury studies in the Cache Creek Watershed, California, 2000–2001: U.S. Geological Survey Water-Resources Investigations Report 03–4335, 30 p., accessed February 24, 2015, at https://water.usgs.gov/pubs/wri/wri034335/.

Domagalski, J.L., Alpers, C.N., Slotton, D.G., Suchanek, T.H., and Ayers, S.M., 2004a, Mercury and methylmercury concentrations and loads in the Cache Creek Basin, California, January 2000 through May 2001: U.S. Geological Survey Scientific Investigations Report 2004–5037, 56 p., accessed February 24, 2015, at https://doi.org/10.3133/sir20045037.

Domagalski, J.L., Alpers, C.N., Slotton, D.G., Suchanek, T.H., and Ayers, S.M., 2004b, Mercury and methylmercury concentrations and loads in the Cache Creek Watershed, California: Science of the Total Environment, v. 327, p. 215–237, accessed February 24, 2015, at https://doi.org/10.1016/j.scitotenv.2004.01.013.

Driscoll, C.T., Mason, R.P., Chan, H.M., Jacob, D.J., and Pirrone, N., 2013, Mercury as a global pollutant: Sources, pathways, and effects: Environmental Science & Technology, v. 47, no. 10, p. 4967–4983, https://pubs.acs.org/doi/abs/10.1021/es305071v.

Fleck, J.A., Marvin-DiPasquale, M., Eagles-Smith, C.A., Ackerman, J.T., Lutz, M.A., Tate, M., Alpers, C.N., Hall, B.D., Krabbenhoft, D.P., and Eckley, C.S., 2016, Mercury and methylmercury in aquatic sediment across western North America: Science of the Total Environment, v. 568, p. 727–738, accessed September 6, 2017, at https://doi.org/10.1016/j.scitotenv.2016.03.044.

Fleming, E.J., Mack, E.E., Green, P.G., and Nelson, D.C., 2006, Mercury methylation from unexpected sources: Molybdate-inhibited freshwater sediments and iron-reducing bacterium: Applied and Environmental Microbiology, v. 72, no. 1, p. 457–464, http://aem.asm.org/content/72/1/457.full.

Foe, C., and Bosworth, D., 2008, Mercury inventory in the Cache Creek Canyon, Staff Report: Rancho Cordova, Calif., Central Valley Regional Water Quality Control Board, 48 p., https://www.waterboards.ca.gov/centralvalley/water_issues/tmdl/central_valley_projects/cache_sulphur_creek/cache_crk_rpt.pdf.

Freepons, D., 1997, Enhancing food production with chitosan seed-coating technology, *in* Goosen, M.F.A., ed., Applications of chitin and chitosan: Boca Raton, Fla., CRC Press, p. 129–139.

Ghernaout, D., and Ghernaout, B., 2012, Sweep flocculation as a second form of charge neutralization—a review: Desalination and Water Treatment, v. 44, nos. 1–3, p. 15–28, https://www.tandfonline.com/doi/abs/10.1080/19443994.2012.691699.

Gilmour, C.C., Henry, E.A., and Mitchell, R., 1992, Sulfate stimulation of mercury methylation in freshwater sediments: Environmental Science & Technology, v. 26, no. 11, p. 2281−2287, https://pubs.acs.org/doi/abs/10.1021/es00035a029.

Gilmour, C.C., Riedel, G.S., Riedel, G., Kwon, S., Landis, R., Brown, S.S., Mensie, C.A., and Ghosh, U., 2013, Activated carbon mitigates mercury and methylmercury bioavailability in contaminated sediments: Environmental Science & Technology, v. 47, no. 22, p. 13001–13010, accessed March 17, 2015, at https://doi.org/10.1021/es4021074.

Goff, F., Bergfeld, D., Kanik, C.J., Counce, D., and Stimac, J.A., 2001, Geochemical data on waters, gases, rocks, and sediments from the Geysers–Clear Lake region, California: Los Alamos National Laboratory, 50 p., https://permalink.lanl.gov/object/tr?what=info:lanl-repo/lareport/LA-13882-MS.

Graham, A.M., Aiken, G.R., and Gilmour, C.C., 2012, Dissolved organic matter enhances microbial mercury methylation under sulfidic conditions: Environmental Science & Technology, v. 46, no. 5, p. 2715−2723, accessed February 24, 2015, at https://doi.org/10.1021/es203658f https://pubs.acs.org/doi/abs/10.1021/es305071v.

Gray, J.E., 2003, Leaching, transport, and methylation of mercury in and around abandoned mercury mines in the Humboldt River Basin and surrounding areas, Nevada: U.S. Geological Survey Bulletin 2210-C, 15 p., https://pubs.usgs.gov/bul/b2210-c/b2210-c-508.pdf.

Gray, J.E., Theodorakos, P.M., Bailey, E.A., and Turner, R.R., 2000, Distribution, speciation, and transport of mercury in stream-sediment, stream-water, and fish collected near abandoned mercury mines in southwestern Alaska, USA: Science of the Total Environment, v. 260, p. 21–33, https://pdfs.semanticscholar.org/f7c0/7bd868d6c5b80f08d33f15ee06e686f19cbd.pdf.

Haitzer, M., Aiken, G.R., and Ryan, J.N., 2002, Binding of mercury(II) to dissolved organic matter: The role of the mercury-to-DOM concentration ratio: Environmental Science & Technology, v. 36, no. 16, p. 3564–3570, https://pubs.acs.org/doi/abs/10.1021/es025699i.

Haitzer, M., Aiken, G.R., and Ryan, J.N., 2003, Binding of mercury(II) to aquatic humic substances: Influence of pH and source of humic substances: Environmental Science & Technology, v. 37, no. 11, p. 2436–2441, https://pubs.acs.org/doi/abs/10.1021/es026291o.

Hall, B.D., Aiken, G.R., Krabbenhoft, D.P., Marvin-DiPasquale, M., and Swarzenski, C.M., 2008, Wetlands as principal zones of methylmercury production in southern Louisiana and the Gulf of Mexico region: Environmental Pollution, v. 154, no. 1, p. 124–134, https://www.ncbi.nlm.nih.gov/pubmed/18242808.

Hansen, A.M., Kraus, T.E.C., Pellerin, B.A., Fleck, J.A., Downing, B.D., and Bergamaschi, B.A., 2016, Optical properties of dissolved organic matter (DOM): Effects of biological and photolytic degradation: Limnology and Oceanography, v. 61, no. 3, p. 1015–1032, https://pubs.er.usgs.gov/publication/70173727.

Henneberry, Y.K., Kraus, T.E.C., Fleck, J.A., Krabbenhoft, D.P., Bachand, P.M., and Horwarth, W.R., 2011, Removal of inorganic mercury and methylmercury from surface waters following coagulation of dissolved organic matter with metal-based salts: Science of the Total Environment, v. 409, no. 3, p. 631–637, accessed February 25, 2015, at https://doi.org/10.1016/j.scitotenv.2010.10.030.

Henneberry, Y.K., Kraus, T.E.C., Nico, P.S., and Horwath, W.R., 2012, Structural stability of coprecipitated natural organic matter and ferric iron under reducing conditions: Organic Geochemistry, v. 48, p. 81–89, accessed September 9, 2017, at https://doi.org/10.1016/j.orggeochem.2012.04.005.

Hsu-Kim, H., Kucharzyk, K.H., Zhang, T., and Deshusses, M.A., 2013, Mechanisms regulating mercury bioavailability for methylating microorganisms in the aquatic environment: A critical review: Environmental Science & Technology, v. 47, no. 6, p. 2441–2456, accessed September 9, 2017, at https://doi.org/10.1021/es304370g.

Hurley, J.P., Benoit, J.M., Babiarz, C.L., Shafer, M.M., Andren, A.W., Sullivan, J.R., Hammond, R., and Webb, D.A., 1995, Influences of watershed characteristics on mercury levels in Wisconsin rivers: Environmental Science & Technology, v. 29, no. 7, p.1867–1875, https://pubs.acs.org/doi/abs/10.1021/es00007a026.

Kerin, E.J., Gilmour, C.C., Roden, E., Suzuki, M.T., Coates, J.D., and Mason, R.P., 2006, Mercury methylation by dissimilatory iron-reducing bacteria: Applied and Environmental Microbiology, v. 72, no. 12, p. 7919–7921, https://www.ncbi.nlm.nih.gov/pmc/articles/PMC1694241/.

Knocke, W.R., and Hemphill, L.H., 1981, Mercury (II) sorption by waste rubber: Water Research, v. 15, no. 2, p. 257–282, https://www.sciencedirect.com/science/article/pii/0043135481901214.

Langner, P., 2009, Investigations of factors controlling mercury release from marine influenced sediments—Grizzly Bay and Liberty Island, California: Freiberg, Germany, Freiberg University of Mining and Technology, M.S. Thesis, 105 p.

Liang, Y., 2016, Chemical and structural characterization of material formed in constructed wetlands treated with metal-based coagulants and their effects on wetland vegetation: Davis, Calif., University of California, Davis: Ph.D. Dissertation, 133 p., http://icpms.ucdavis.edu/application/files/8815/3609/6560/Chemical_and_Structural_Charac.pdf.

Lui, C., and Bai, R., 2014, Recent advances in chitosan and its derivatives as adsorbents for removal of pollutants from water and wastewater: Current Opinion in Chemical Engineering, v. 4, p. 62–70, accessed February 24, 2015, at https://doi.org/10.1016/j.coche.2014.01.004.

Macpherson, J., 2004, Storm-Klear™ (Chitosan) toxicity and applications: Microsoft PowerPoint on-line, accessed March 14, 2017, at http://www.waterboards.ca.gov/water_issues/programs/stormwater/docs/advtreat/naturalsitesolutions.pdf.

Marineau, M.D., and Wright, S.A., 2017, Bed-material characteristics of the Sacramento–San Joaquin Delta, California, 2010–13: U.S. Geological Survey Data Series 1026, 55 p., accessed March 12, 2017, at https://doi.org/10.3133/ds1026.

Mehrotra, A.S., Horne, A.J., and Sedlak, D.L., 2003, Reduction of net mercury methylation by iron in *desulfobulbus propionicus* (1pr3) cultures: Implications for engineered wetlands: Environmental Science & Technology, v. 37, no. 13, p. 3018–3023, https://pubs.acs.org/doi/abs/10.1021/es0262838.

Miretzky, P., and Cirelli, A.F., 2009, Hg(II) removal from water by chitosan and chitosan derivatives—A review: Journal of Hazardous Materials, v. 167, nos. 1–3, p. 10–23, accessed March 17, 2015, at https://doi.org/10.1016/j.jhazmat.2009.01.060.

Morel, F.M., Kraepiel, A.M., and Amyot, M., 1998, The chemical cycle and bioaccumulation of mercury: Annual Review of Ecology Systematics, v. 29, p. 543–566, http://www.esf.edu/efb/mitchell/Class%20Readings%5CAnnRevEcoSys29.543.566.pdf.

Osifo, P.O., Neomagus, H.W.J.P., Everson, R.C., Webster, A., and Gun, M.A., 2009, The adsorption of copper in a packed-bed of chitosan beads: Modeling, multiple adsorption and regeneration: Journal of Hazardous Materials, v. 167, nos. 1–3, p. 1242–1245, accessed October 12, 2016, at https://doi.org/10.1016/j.jhazmat.2009.01.109.

Poppe, L.J., Eliason, A.H., Fredericks, J.J., Rendigs, R.R., Blackwood, D., and Polloni, C.F., 2000, Grain size analysis of marine sediments: Methodology and data processing, *in* Poppe, L.J., and Polloni, C.F., eds., USGS east-coast sediment analysis: Procedures, database, and georeferenced displays: U.S. Geological Survey Open-File Report 00–358, CD-ROM, https://doi.org/10.3133/ofr00358.

Randall, P.M., and Chattopadhyay, S., 2013, Mercury contaminated sediment sites—An evaluation of remedial options: Environmental Research, v. 125, p. 131–149, accessed February 24, 2015, at https://www.sciencedirect.com/science/article/pii/S0013935113000133.

Rytuba, J.J., 2000, Mercury mine drainage and processes that control its environmental impact: Science of the Total Environment, v. 260, nos. 1–3, p. 57–71, https://www.ncbi.nlm.nih.gov/pubmed/11032116.

Rytuba, J.J., Hothem, R.L., Brussee, B.E., and Goldstein, D.N., 2011, Impact of mine and natural sources of mercury on water, sediment, and biota in Harley Gulch adjacent to the Abbott-Turkey Run mine, Lake County, California: U.S. Geological Survey Open File Report 2011–1265, 105 p., accessed September 9, 2016, at https://pubs.usgs.gov/of/2011/1265/.

Sibiya, S.M., 2014, Evaluation of the streaming current detector (SCD) for coagulation control: Procedia Engineering, v. 70, p. 1211–1220, https://www.sciencedirect.com/science/article/pii/S1877705814001362.

St. Louis, V.L., Rudd, J.W., Kelly, C.A., Bodaly, R.A., Paterson, M.J., Beaty, K.G., Hesslein, R.H., Heyes, A., and Majewski, A.R., 2004, The rise and fall of mercury methylation in an experimental reservoir: Environmental Science & Technology, v. 38, no. 5, p. 1348–58, https://www.ncbi.nlm.nih.gov/pubmed/15046335.

Stumpner, E.B., Kraus, T.E.C., Fleck, J.A., Hansen, A.M., Bachand, S.M., Horwath, W.R., DeWild, J.F., Krabbenhoft, D.P., and Bachand, P.A.M., 2015, Mercury, monomethyl mercury, and dissolved organic carbon concentrations in surface water entering and exiting constructed wetlands treated with metal-based coagulants, Twitchell Island, California: U.S. Geological Survey Data Series 950, 26 p., accessed June 17, 2016, at https://dx.doi.org/10.3133/ds950.

Suchanek, T.H., Slotton, D.G., Nelson, D.C., Ayers, S.M., Asher, C., Weyand, R., Liston, A., and Eagles-Smith, C., 2002, Mercury loading and source bioavailability from the upper Cache Creek mining districts: Assessment of ecological and human health impacts of mercury in the San Francisco Bay–Delta Watershed: CALFED, p. 72, https://www.researchgate.net/publication/237333169_MERCURY_LOADING_AND_SOURCE_BIOAVAILABILITY_FROM_THE_UPPER_CACHE_CREEK_MINING_DISTRICTS.

Taylor, H.E., Antweiler, R.C., Roth, D.A., Alpers, C.N., and Dileanis, P., 2012, Selected trace elements in the Sacramento River, California: Occurrence and distribution: Archives of Environmental Contamination and Toxicology, v. 62, no. 4, p. 557–569, accessed June 17, 2016, at http://dx.doi.org/10.1007/s00244-011-9738-z.

Ulrich, P.D., and Sedlak, D.L., 2010, Impact of iron amendment on net methylmercury export from tidal wetland microcosms: Environmental Science & Technology, v. 44, no. 19, p. 7659–7665, https://pubs.acs.org/doi/abs/10.1021/es1018256.

U.S. Environmental Protection Agency, 1999, Method 1631, Mercury in water by oxidation, purge and trap, and cold vapor atomic fluorescence spectrometry (revision B): Washington, D.C., U.S. Environmental Protection Agency, no. EPA-821-R-99-005, 31 p.

U.S. Environmental Protection Agency, 2005, Method 415.3, Determination of total organic carbon and specific UV absorbance at 245 nm in source water and drinking water (revision 1.1): U.S. Environmental Protection Agency, no. EPA/600/R-05/055, 56 p.

U.S. Geological Survey, 2012, The national field manual for the collection of water-quality data (version 7): U.S. Geological Survey Techniques and Method, book 9, chaps. A1–A9, accessed April 5, 2013, at accessed June 17, 2016, at https://water.usgs.gov/owq/FieldManual/.

Wiener, J.G., Krabbenhoft, D.P., Heinz, G.H., and Scheuhammer, A.M., 2003, Ecotoxicology of mercury, *in* Hoffman, D.J., Rattner, B.A., Burton, G.A., Jr., and Cairns, J., Jr., eds., Handbook of ecotoxicology (2d ed.): Boca Raton, Fla., Lewis Publishers, p. 409–463, https://pubs.er.usgs.gov/publication/5211201.

Wilde, F.D., Radtke, D.B., Gibs, J., and Iwatsubo, R.T., eds., 2004. Processing of water samples (ver. 2.2, with updates through 2009): U.S. Geological Survey Techniques of Water-Resources Investigations, book 9, chap. A5, 26 p., accessed March 10, 2017, at http://pubs.water.usgs.gov/twri9A5/.

Wood, M.L., Foe, C.G., Cooke, J., Louie, S.J., and Bosworth, D.H., 2010, Sacramento–San Joaquin Delta Estuary TMDL for methylmercury—Staff Report California Environmental Protection Agency, Regional Water Quality Control Board, Central Valley Region, 376 p., https://www.waterboards.ca.gov/rwqcb5/water_issues/tmdl/central_valley_projects/delta_hg/archived_delta_hg_info/april_2010_hg_tmdl_hearing/apr2010_tmdl_staffrpt_final.pdf.

Appendix Tables

Table 1–1. Mercury and dissolved organic-carbon concentration data, and optical data from samples and blanks collected during the 'clean' portion of the coagulation full experiment.

[All mercury analysis performed at the U.S. Geological Survey (USGS) Wisconsion Mercury Research Laboratory. Each sample was analyzed twice, both results are reported. All optical and dissolved organic carbon (DOC) analysis performed at the USGS California Water Science Center Organic Matter Research Laboratory. Numbers at the end of each sample ID note the dose amount. Blank samples were selected at random to be tested and noted with lowercase letters. **Abbreviations**: A_{254}, absorbance at 254 nanometers; nm, nanometers; FI, flourescence index; ID, identification; L mg C^{-1} m^{-1}, liters per milligram of carbon per meter; MeHg, methylmercury; mg/L, milligrams per liter; mm/dd/yyyy, month/day/year; N/A, not applicable; ng/L, nanograms per liter; RFE, relative fluorescent efficiency; RU, Raman units; $SUVA_{254}$, specific ultraviolet absorbance at 254 nanometers; THg, total mercury; TM, trademark; <, less than]

Sample ID	Date (mm/dd/yyyy)	Methyl mercury (ng/L)		Total mercury (ng/L)		A_{254} (nm)	DOC (mg/L)	$SUVA_{254}$ (L mg C^{-1} m^{-1})	RFE (RU)	FI
		MeHg - 1	MeHg - 2	THg - 1	THg - 2					
ChitoVan™										
Hg clean_control	03/24/2016	0.38	0.37	33.20	41.50	0.14	4.78	3.01	18.47	1.63
Hg clean_20	03/24/2016	0.15	0.15	9.69	10.40	0.13	4.88	2.71	22.10	1.65
Hg clean_30	03/24/2016	0.15	0.14	9.43	9.85	0.13	4.94	2.69	22.20	1.64
Hg clean_50	03/24/2016	0.13	0.14	7.42	8.22	0.13	5.03	2.60	22.91	1.64
Hg clean_120	03/24/2016	0.11	0.11	6.32	6.74	0.13	5.31	2.46	22.69	1.64
Ferralyte™										
Hg clean_control	03/24/2016	0.40	0.30	42.80	36.60	0.14	4.77	3.00	18.70	1.62
Hg clean_20	03/24/2016	0.21	0.19	22.40	22.90	0.12	4.40	2.74	20.85	1.67
Hg clean_40	03/24/2016	0.16	0.15	15.00	13.20	0.11	4.05	2.64	22.03	1.68
Hg clean_60	03/24/2016	0.12	0.13	7.26	7.58	0.09	3.72	2.35	25.91	1.71
Hg clean_100	03/24/2016	0.09	0.09	5.29	5.08	0.07	3.34	2.12	28.96	1.73
Ultrion™										
Hg clean_control	03/28/2016	0.40	0.41	45.40	41.40	0.15	4.79	3.12	16.48	1.64
Hg clean_20	03/28/2016	0.22	0.04	2.37	2.12	0.07	3.42	2.01	35.83	1.81
Hg clean_40	03/28/2016	<0.04	<0.04	3.14	4.10	0.05	2.89	1.78	38.43	1.85
Hg clean_60	03/28/2016	0.05	0.05	4.03	4.06	0.05	2.66	1.72	39.69	1.88
Hg clean_100	03/28/2016	<0.04	0.04	2.80	2.68	0.05	3.30	1.52	28.74	1.83
Coagulation experiment blanks										
Hg clean_Blank_chitovan	03/24/2016	<0.04	<0.04	0.30	0.22	N/A	0.19	N/A	N/A	N/A
Hg clean_Blank_ferralyte	03/24/2016	<0.04	<0.04	0.43	0.44	N/A	0.14	N/A	N/A	N/A
Hg clean_Blank_ultrion	03/28/2016	<0.04	<0.04	0.61	0.65	N/A	0.20	N/A	N/A	N/A

Table 2–1. Mercury concentrations and dissolved organic-carbon concentrations for samples and blanks collected during the sorbent experiment.

[All mercury analysis performed at the U.S. Geological Survey (USGS) Wisconsin Water Science Center Mercury Research Laboratory. All dissolved organic carbon (DOC) analysis performed at the USGS California Water Science Center Organic Matter Research Laboratory. Letters assigned to each sample represent the total amount of water that passed through the Teflon in-line filter: 500 mL (A), 1500 mL (C), and 3000 mL (F), blank samples were selected at random to be tested and noted with lowercase letters. **Abbreviations**: L/min, liters per minute; mg/L, milligrams per liter; mL, milliliter; mm/dd/yyyy, month/day/year; N/A, not applicable; ng/L, nanograms per liter; OFW, organic-free water; <, less than; —, no sample data exists]

Source	Sorbent	Rate (L/min)	Run	Collection date (mm/dd/yyyy)	Methyl mercury (ng/L)	Total mercury (ng/L)	DOC (mg/L)
				Chitosan			
Turkey Creek	chitosan	0.1	A	05/04/2016	—	133	—
Turkey Creek	chitosan	0.1	B	05/04/2016	—	127	—
Turkey Creek	chitosan	0.1	C	05/04/2016	—	138	—
Turkey Creek	chitosan	0.1	E	05/04/2016	—	129	—
Turkey Creek	chitosan	0.1	F	05/04/2016	—	151	—
Turkey Creek	chitosan	0.5	A	05/04/2016	—	136	—
Turkey Creek	chitosan	0.5	F	05/04/2016	—	134	—
Turkey Creek	chitosan	1	A	05/04/2016	—	187	—
Turkey Creek	chitosan	1	F	05/04/2016	—	196	—
Connate Spring	chitosan	0.1	A	05/04/2016	—	160	—
Connate Spring	chitosan	0.1	B	05/04/2016	—	157	—
Connate Spring	chitosan	0.1	C	05/04/2016	—	163	—
Connate Spring	chitosan	0.1	E	05/04/2016	—	158	—
Connate Spring	chitosan	0.1	F	05/04/2016	—	170	—
Connate Spring	chitosan	0.5	A	05/04/2016	—	192	—
Connate Spring	chitosan	0.5	F	05/04/2016	—	202	—
Connate Spring	chitosan	1	A	05/04/2016	—	181	—
Connate Spring	chitosan	1	F	05/04/2016	—	174	—
				Coconut			
Turkey Creek	coconut	0.1	A	05/04/2016	—	146	—
Turkey Creek	coconut	0.1	B	05/04/2016	—	141	—
Turkey Creek	coconut	0.1	C	05/04/2016	—	159	—
Turkey Creek	coconut	0.1	E	05/04/2016	—	153	—
Turkey Creek	coconut	0.1	F	05/04/2016	—	183	—
Turkey Creek	coconut	0.5	A	05/04/2016	—	147	—
Turkey Creek	coconut	1	F	05/04/2016	—	382	—
Connate Spring	coconut	0.1	A	05/04/2016	—	136	—
Connate Spring	coconut	0.1	B	05/04/2016	—	140	—
Connate Spring	coconut	0.1	C	05/04/2016	—	165	—
Connate Spring	coconut	0.1	E	05/04/2016	—	148	—
Connate Spring	coconut	0.1	F	05/04/2016	—	165	—
Connate Spring	coconut	0.5	A	05/04/2016	—	204	—
Connate Spring	coconut	0.5	F	05/04/2016	—	222	—
Connate Spring	coconut	1	A	05/04/2016	—	161	—
Connate Spring	coconut	1	F	05/04/2016	—	210	—

Table 2–1. Mercury concentrations and dissolved organic-carbon concentrations for samples and blanks collected during the sorbent experiment.—Continued

[All mercury analysis performed at the U.S. Geological Survey (USGS) Wisconsin Water Science Center Mercury Research Laboratory. All dissolved organic carbon (DOC) analysis performed at the USGS California Water Science Center Organic Matter Research Laboratory. Letters assigned to each sample represent the total amount of water that passed through the Teflon in-line filter: 500 mL (A), 1500 mL (C), and 3000 mL (F), blank samples were selected at random to be tested and noted with lowercase letters. **Abbreviations**: L/min, liters per minute; mg/L, milligrams per liter; mL, milliliter; mm/dd/yyyy, month/day/year; N/A, not applicable; ng/L, nanograms per liter; OFW, organic-free water; <, less than; —, no sample data exists]

Source	Sorbent	Rate (L/min)	Run	Collection date (mm/dd/yyyy)	Methyl mercury (ng/L)	Total mercury (ng/L)	DOC (mg/L)
Coal							
Turkey Creek	coal	0.1	A	05/05/2016	—	116	—
Turkey Creek	coal	0.1	B	05/05/2016	—	108	—
Turkey Creek	coal	0.1	C	05/05/2016	—	119	—
Turkey Creek	coal	0.1	E	05/05/2016	—	116	—
Turkey Creek	coal	0.1	F	05/05/2016	—	132	—
Turkey Creek	coal	0.5	A	05/05/2016	—	140	—
Turkey Creek	coal	0.5	F	05/05/2016	—	150	—
Turkey Creek	coal	1	A	05/05/2016	—	147	—
Turkey Creek	coal	1	F	05/05/2016	—	159	—
Connate Spring	coal	0.1	A	05/05/2016	—	148	—
Connate Spring	coal	0.1	B	05/05/2016	—	138	—
Connate Spring	coal	0.1	C	05/05/2016	—	151	—
Connate Spring	coal	0.1	E	05/05/2016	—	159	—
Connate Spring	coal	0.1	F	05/05/2016	—	159	—
Connate Spring	coal	0.5	A	05/05/2016	—	164	—
Connate Spring	coal	0.5	F	05/05/2016	—	158	—
Connate Spring	coal	1	A	05/05/2016	—	171	—
Connate Spring	coal	1	F	05/05/2016	—	171	—
Untreated samples							
Turkey Creek	none	none	Raw	05/04/2016	0.04	176	3.04
Turkey Creek	none	none	Raw	05/05/2016	0.04	159	2.81
Connate Spring	none	none	Raw	05/04/2016	0.04	325	5.41
Connate Spring	none	none	Raw	05/05/2016	0.05	182	5.71
Sorbent experiment blanks							
OFW blank	none	none	N/A	05/05/2016	—	—	0.25
Blank_glass beads	none	none	N/A	05/05/2016	<0.04	0.26	—
Blank_glass beads	none	none	N/A	05/05/2016	2.10	0.17	—
Blank_glass beads	none	none	N/A	05/05/2016	<0.04	0.47	—

Table 3–1. Selected water-quality measurements collected during the coagulation test run and the coagulation full experiment, by elapsed settling time.

[All experiments were performed at the U.S. Geological Survey California Water Science Center. **Abbreviations**: cm, centimeters; fDOM, fluorescent dissolved organic matter; FNU, Formazin Nephelometric Units; L, liters; mL, milliliters; µS, microsiemens; N/A, not applicable; QSU, quinine sulfate units; —, no data exists; µL, microliters]

Coagulant test run								
Sample ID	Coagulant	Water added (mL)	Dose amount (µL)	Dose rate (µL/L)	Time: 5 minutes, settling	Time: 10 minutes, settling	Time: 20 minutes, settling	Time: 30 minutes, settling
					Turbidity (FNU)	Turbidity (FNU)	Turbidity (FNU)	Turbidity (FNU)
CCSB- RAW	NA	—	—	0.0	1,308	1,308	1,308	1,308
CCSB-A	ChitoVan™	606.4	20	33	245.2	197	176	171.3
CCSB-B	ChitoVan™	605.8	60	99	38.5	26.6	26.32	24
CCSB-C	ChitoVan™	605.4	100	165	28.67	21.8	7.57	16.9
CCSB-D	ChitoVan™	605.4	140	231	15.6	15.5	7	6.58
CCSB-E	ChitoVan™	609	180	296	15.64	9.8	6	7.65

Coagulation full experiment (dirty stage)																
Sample ID	Coagulant	Water added (mL)	Dose amount (µL)	Dose rate (µL/L)	Time: 0 minutes				Time: 5 minutes settling				Time: 10 minutes settling			
					pH	SpC (µS/cm)	Turbidity (FNU)	fDOM (QSE)	pH	SpC (µS/cm)	Turbidity (FNU)	fDOM (QSE)	pH	SpC (µS/cm)	Turbidity (FNU)	fDOM (QSE)
CCSB Chitovan_”dirty”	ChitoVan™	996	1	1	8.09	388	310	12.9	8.03	382	281	13.4	7.89	376	250	14.6
CCSB Chitovan_”dirty”	ChitoVan™	978	20	20	8.03	386	300	15.4	8	382	160	25.8	7.87	370	130	27.15
CCSB Chitovan_”dirty”	ChitoVan™	988	30	30	8.04	385	330	13.6	7.94	383	100	31.25	7.98	371	88.5	32.5
CCSB Chitovan_”dirty”	ChitoVan™	986	40	41	8.03	386	300	10.3	7.88	379	83	35.53	7.9	370	81.5	34.4
CCSB Chitovan_”dirty”	ChitoVan™	978	50	51	8.05	386	330	11.1	7.92	376	72	37.15	7.89	372	62.3	35.5
CCSB Chitovan_”dirty”	ChitoVan™	996	60	60	8.05	386	300	14.9	7.89	382	81	35	7.87	367	76.5	33.8
CCSB Chitovan_”dirty”	ChitoVan™	996	120	120	—	—	—	—	7.89	373	77	32	7.88	378	81	31.3
CCSB Ferric Sulfate_”dirty”	Ferralyte™	988	1	1	7.96	379	330	11.9	8.22	388	300	13.7	8.03	387	260	15.1
CCSB Ferric Sulfate_”dirty”	Ferralyte™	996	20	20	7.95	385	330	13.5	7.85	389	195	16.4	7.86	357	131	22.5
CCSB Ferric Sulfate_”dirty”	Ferralyte™	998	40	40	7.96	387	320	12.8	7.71	379	132	18.7	7.71	377	62	24.5
CCSB Ferric Sulfate_”dirty”	Ferralyte™	990	60	61	8.03	386	330	12.1	7.42	385	45	22.8	7.5	361	33	22.8
CCSB Ferric Sulfate_”dirty”	Ferralyte™	996	80	80	8.02	386	300	12.9	7.35	365	28	19	7.35	387	25	22
CCSB Ferric Sulfate_”dirty”	Ferralyte™	998	100	100	8.02	385	320	12.7	7.15	398	21	20.5	7.21	382	18	16.5
CCSB AlClOH_”dirty”	Ultrion™	996	1	1	7.6	386	330	14.6	7.73	392	307	13.5	7.6	374	310	14.2
CCSB AlClOH_”dirty”	Ultrion™	988	20	20	7.46	386	350	13.7	7.78	374	9	26.5	7.71	379	6.6	26
CCSB AlClOH_”dirty”	Ultrion™	990	40	40	7.7	384	330	13.3	7.56	372	27	21	7.68	376	11.5	22.6
CCSB AlClOH_”dirty”	Ultrion™	998	60	60	7.9	385	300	13.8	7.51	375	36	22.5	7.64	375	21.4	23.5
CCSB AlClOH_”dirty”	Ultrion™	992	80	81	7.9	384	320	12.1	7.59	380	26	25.3	7.63	376	16.5	25.4
CCSB AlClOH_”dirty”	Ultrion™	996	100	100	7.9	386	300	13.5	7.52	389	18	24.1	7.56	386	11.7	27.8

Table 3–1. Selected water-quality measurements collected during the coagulation test run and the coagulation full experiment, by elapsed settling time.—Continued

[All experiments were performed at the U.S. Geological Survey California Water Science Center. **Abbreviations**: cm, centimeters; fDOM, fluorescent dissolved organic matter; FNU, Formazin Nephelometric Units; L, liters; mL, milliliters; µS, microsiemens; N/A, not applicable; QSU, quinine sulfate units; —, no data exists; µL, microliters]

Coagulation full experiment (dirty stage)—Continued												
Sample ID	Coagulant	Water added (mL)	Dose amount (µL)	Dose rate (µL/L)	Time: 20 minutes settling				Time: 30 minutes settling			
					pH	SpC (µS/cm)	Turbidity (FNU)	fDOM (QSE)	pH	SpC (µS/cm)	Turbidity (FNU)	fDOM (QSE)
CCSB Chitovan_"dirty"	ChitoVan™	996	1	1	7.88	380	270	14.5	7.82	373	270	16.1
CCSB Chitovan_"dirty"	ChitoVan™	978	20	20	7.84	377	109	29.3	7.82	364	96	29.6
CCSB Chitovan_"dirty"	ChitoVan™	988	30	30	7.85	380	82	33.4	7.87	375	76	34.1
CCSB Chitovan_"dirty"	ChitoVan™	986	40	41	7.85	373	76	32.2	7.81	374	72	35
CCSB Chitovan_"dirty"	ChitoVan™	978	50	51	7.83	364	63	35.5	7.87	380	61	34.5
CCSB Chitovan_"dirty"	ChitoVan™	996	60	60	7.82	377	75	35.4	7.89	360	75	34.8
CCSB Chitovan_"dirty"	ChitoVan™	996	120	120	7.96	367	73	32.5	8.01	364	64	33.3
CCSB Ferric Sulfate_"dirty"	Ferralyte™	988	1	1	7.9	384	250	13	7.8	385	240	15.1
CCSB Ferric Sulfate_"dirty"	Ferralyte™	996	20	20	7.85	357	102	22.7	7.85	360	82	25.3
CCSB Ferric Sulfate_"dirty"	Ferralyte™	998	40	40	7.65	374	60	23.5	7.6	372	52	26
CCSB Ferric Sulfate_"dirty"	Ferralyte™	990	60	61	7.4	384	21	25	7.45	371	22	26.4
CCSB Ferric Sulfate_"dirty"	Ferralyte™	996	80	80	7.25	374	21	18.5	7.3	378	18	21
CCSB Ferric Sulfate_"dirty"	Ferralyte™	998	100	100	7.1	370	13	21.4	7.15	372	10	22.5
CCSB AlClOH_"dirty"	Ultrion™	996	1	1	7.69	384	260	14.1	7.73	367	250	16.4
CCSB AlClOH_"dirty"	Ultrion™	988	20	20	7.77	365	5	25.5	7.77	368	4	24.5
CCSB AlClOH_"dirty"	Ultrion™	990	40	40	7.75	376	11	22.4	7.74	379	9	21.8
CCSB AlClOH_"dirty"	Ultrion™	998	60	60	7.57	380	17	18.7	7.63	375	15	21.2
CCSB AlClOH_"dirty"	Ultrion™	992	80	81	7.62	384	16	26	7.64	379	12	25.9
CCSB AlClOH_"dirty"	Ultrion™	996	100	100	7.61	383	9	22.5	7.61	388	6	25.9

Table 3–1. Selected water-quality measurements collected during the coagulation test run and the coagulation full experiment, by elapsed settling time.—Continued

[All experiments were performed at the U.S. Geological Survey California Water Science Center. **Abbreviations**: cm, centimeters; fDOM, fluorescent dissolved organic matter; FNU, Formazin Nephelometric Units; L, liters; mL, milliliters; µS, microsiemens; N/A, not applicable; QSU, quinine sulfate units; —, no data exists; µL, microliters]

Coagulation full experiment (clean stage)					
Sample ID	**Coagulant**	**Water added (mL)**	**Dose amount (µL)**	**Dose rate (µL/L)**	**Hach Turbidity (FNU)**
CCSB Chitovan_Hg clean_control	N/A	1,000	0	0	335
CCSB Chitovan_Hg clean_20	ChitoVan™	974	20	21	50.2
CCSB Chitovan_Hg clean_30	ChitoVan™	966	30	31	48.1
CCSB Chitovan_Hg clean_50	ChitoVan™	996	50	50	37.5
CCSB Chitovan_Hg clean_120	ChitoVan™	994	120	121	28.5
CCSB Chitovan_Hg clean_Blank	N/A	984	N/A	N/A	0.046
CCSB Ferric Sulfate_Hg clean_control	N/A	996	0	0	337
CCSB Ferric Sulfate_Hg clean_20	Ferralyte™	992	20	20	155
CCSB Ferric Sulfate_Hg clean_40	Ferralyte™	998	40	40	81
CCSB Ferric Sulfate_Hg clean_60	Ferralyte™	996	60	60	39.3
CCSB Ferric Sulfate_Hg clean_100	Ferralyte™	998	100	100	23.2
CCSB Ferric Sulfate_Hg clean_Blank	N/A	998	N/A	N/A	0.044
CCSB AlClOH_Hg clean_control	N/A	998	0	0	354
CCSB AlClOH_Hg clean_20	Ultrion™	986	20	20	4.86
CCSB AlClOH_Hg clean_40	Ultrion™	996	40	40	10.6
CCSB AlClOH_Hg clean_60	Ultrion™	1000	60	60	18
CCSB AlClOH_Hg clean_100	Ultrion™	992	100	101	9.65
CCSB AlClOH_Hg clean_Blank	N/A	998	N/A	N/A	0.065

Table 4–1. Data for least squares means (+/– std error) for total mercury (THg) removed using a linear fixed effects model including source water, sorbent type, and flow rate as fixed effects (r2=0.86; p < 0.0001).

[L/min, liters per minute; ng, nanograms; std, standard; +/-, plus or minus; <, less than]

Sorbent	Flow rate (L/min)	Source	Least square mean (ng)	Standard error (ng)
Chitosan	0.1	Connate Spring	12.12	2.32
Chitosan	0.5	Connate Spring	–5.46	3.66
Chitosan	1.0	Connate Spring	4.32	3.66
Coal	0.1	Connate Spring	16.72	2.32
Coal	0.5	Connate Spring	10.54	3.66
Coal	1.0	Connate Spring	5.57	3.66
Coconut	0.1	Connate Spring	17.52	2.32
Coconut	0.5	Connate Spring	–13.46	3.66
Coconut	1.0	Connate Spring	0.32	3.66
Chitosan	0.1	Turkey Creek	20.90	2.61
Chitosan	0.5	Turkey Creek	20.54	3.66
Chitosan	1.0	Turkey Creek	–7.68	3.66
Coal	0.1	Turkey Creek	13.32	2.32
Coal	0.5	Turkey Creek	7.04	3.66
Coal	1.0	Turkey Creek	3.07	3.66
Coconut	0.1	Turkey Creek	9.72	2.32
Coconut	0.5	Turkey Creek	10.79	3.66
Coconut	1.0	Turkey Creek	–20.08	5.42

Table 5–1. Data for amount of total mercury removed at the 0.1 liters per minute (L/min) flow rate for samples collected during the sorbent experiment.

[L, liters; ng, nanograms; —, no data]

Sorbent	Flow rate (L/min)	Source	Volume passed (L)	Cumulative mercury removed (ng)
Chitosan	0.1	Turkey Creek	0	—
Chitosan	0.1	Turkey Creek	0.5	—
Chitosan	0.1	Turkey Creek	1	24.5
Chitosan	0.1	Turkey Creek	1.5	43.5
Chitosan	0.1	Turkey Creek	2	60.4
Chitosan	0.1	Turkey Creek	2.5	83.9
Chitosan	0.1	Turkey Creek	3	96.4
Coconut	0.1	Turkey Creek	0	—
Coconut	0.1	Turkey Creek	0.5	15.0
Coconut	0.1	Turkey Creek	1	32.5
Coconut	0.1	Turkey Creek	1.5	41.0
Coconut	0.1	Turkey Creek	2	45.5
Coconut	0.1	Turkey Creek	2.5	57.0
Coconut	0.1	Turkey Creek	3	53.5
Coal	0.1	Turkey Creek	0	—
Coal	0.1	Turkey Creek	0.5	21.5
Coal	0.1	Turkey Creek	1	30.5
Coal	0.1	Turkey Creek	1.5	50.5
Coal	0.1	Turkey Creek	2	68.4
Coal	0.1	Turkey Creek	2.5	71.4
Coal	0.1	Turkey Creek	3	84.9
Chitosan	0.1	Connate Spring	0	—
Chitosan	0.1	Connate Spring	0.5	13.0
Chitosan	0.1	Connate Spring	1	26.0
Chitosan	0.1	Connate Spring	1.5	37.5
Chitosan	0.1	Connate Spring	2	47.8
Chitosan	0.1	Connate Spring	2.5	53.6
Chitosan	0.1	Connate Spring	3	61.6
Coconut	0.1	Connate Spring	0	—
Coconut	0.1	Connate Spring	0.5	25.0
Coconut	0.1	Connate Spring	1	44.5
Coconut	0.1	Connate Spring	1.5	55.0
Coconut	0.1	Connate Spring	2	65.5
Coconut	0.1	Connate Spring	2.5	72.9
Coconut	0.1	Connate Spring	3	83.4
Coal	0.1	Connate Spring	0	—
Coal	0.1	Connate Spring	0.5	17.0
Coal	0.1	Connate Spring	1	35.2
Coal	0.1	Connate Spring	1.5	50.7
Coal	0.1	Connate Spring	2	64.8
Coal	0.1	Connate Spring	2.5	73.1
Coal	0.1	Connate Spring	3	84.6

Table 6–1. Trace metal concentrations for sorbent experiment samples and source waters.

[All trace metal analysis performed at the U.S. Geological Survey Trace Metals Research Laboratory in Boulder, CO. **Abbreviations**: OR, sample was above instrument calibration limit; µg/L, micrograms per liter; <, less than. Letters assigned to each sample represent the total amount of water passed through the filter: 500 mL (A), 1,500 mL (C), and 3,000 mL (F), blank samples were selected at random to be tested and noted with lowercase letters.]

Sample ID	Collection date (mm/dd/yyyy)	Al	As	B	Ba	Be	Bi	Ca	Cd	Ce	Co	Cr	Cu	Dy	Er	Eu	Fe	Ga	Gd
Untreated Source Water (µg/L)																			
Turkey Creek	05/04/2016	44	<22	OR	79	0.009	0.31	29	0.06	0.13	1.2	6.3	4.2	0.033	0.026	0.001	11	0.067	0.018
Turkey Creek	05/05/2016	44	<22	OR	73	0.011	0.13	27	0.41	0.18	1.1	5.6	7.3	0.029	0.023	<0.0002	25	0.025	0.009
Connate Spring	05/04/2016	65	<22	OR	42	0.007	0.28	42	0.48	0.083	0.68	5.7	5.6	0.014	0.011	<0.0002	80	0.027	0.006
Connate Spring	05/05/2016	26	<22	OR	39	0.006	0.18	42	0.1	0.043	0.43	4.5	3.7	0.011	0.009	<0.0002	16	0.017	0.007
Chitosan (µg/L)																			
Turkey Creek-A	05/04/2016	39	<22	OR	81	0.009	0.05	32	0.03	0.12	1.2	6.3	5.4	0.027	0.021	<0.0002	15	0.027	0.009
Turkey Creek-C	05/04/2016	34	<22	OR	82	0.013	0.22	34	0.12	0.1	1.3	5.6	8.6	0.029	0.022	<0.0002	38	0.032	0.019
Turkey Creek-F	05/04/2016	34	<22	OR	80	0.013	0.35	31	0.15	0.1	1.3	6.1	13	0.033	0.023	<0.0002	10	0.039	0.018
Connate Spring-A	05/04/2016	22	<22	OR	43	0.004	0.26	46	0.12	0.034	0.54	5.4	4.7	0.009	0.011	<0.0002	16	0.018	0.006
Connate Spring-C	05/04/2016	22	<22	OR	41	0.004	0.11	44	0.06	0.039	0.51	5.5	4	0.010	0.008	<0.0002	11	0.017	0.003
Connate Spring-F	05/04/2016	21	<22	OR	41	0.004	0.14	41	0.03	0.037	0.50	5.3	4.2	0.011	0.010	<0.0002	10	0.016	0.005
Coconut (µg/L)																			
Turkey Creek-A	05/04/2016	37	<22	OR	85	0.018	1	31	0.48	0.12	1.3	6.4	3.9	0.032	0.025	0.001	25	0.074	0.026
Turkey Creek-C	05/04/2016	34	<22	OR	80	0.017	0.06	30	0.06	0.11	1.2	6	4.7	0.031	0.025	<0.0002	11	0.032	0.018
Turkey Creek-F	05/04/2016	32	<22	OR	79	0.012	0.56	28	0.08	0.11	1.2	5.9	8.1	0.032	0.022	<0.0002	34	0.026	0.019
Connate Spring-A	05/04/2016	25	<22	OR	45	0.005	0.12	41	0.03	0.04	0.52	5.6	3.9	0.01	0.011	<0.0002	19	0.02	0.005
Connate Spring-C	05/04/2016	26	<22	OR	45	0.003	0.28	44	0.04	0.04	0.55	5.6	5	0.012	0.01	<0.0002	16	0.018	0.006
Connate Spring-F	05/04/2016	25	<22	OR	42	0.004	0.31	45	0.11	0.04	0.51	8.9	3.7	0.011	0.012	<0.0002	19	0.02	0.007
Coal (µg/L)																			
Turkey Creek-A	05/05/2016	50	<22	OR	77	0.015	0.24	33	0.15	0.17	1.1	6.5	3.9	0.05	0.046	0.001	16	0.32	0.019
Turkey Creek-C	05/05/2016	39	<22	OR	78	0.015	0.12	33	0.04	0.13	0.96	5.8	4.4	0.037	0.037	<0.0002	15	0.13	0.023
Turkey Creek-F	05/05/2016	37	<22	OR	76	0.017	0.15	34	0.30	0.13	1.1	6.4	4.2	0.04	0.028	<0.0002	14	0.087	0.019
Connate Spring-A	05/05/2016	36	<22	OR	42	0.004	0.13	42	0.04	0.07	0.51	6	9.1	0.019	0.018	<0.0002	16	0.26	0.01
Connate Spring-C	05/05/2016	55	<22	OR	42	0.006	0.12	43	0.64	0.06	0.55	6.3	4.7	0.016	0.014	<0.0002	27	0.14	0.008
Connate Spring-F	05/05/2016	28	<22	OR	42	0.004	0.23	43	0.30	0.06	0.54	5.9	4.5	0.014	0.014	0.001	13	0.1	0.004
Blanks (µg/L)																			
Blank - a	05/05/2016	2.9	<22	<137	0.1	0.003	0.32	0.05	0.03	0.01	0.028	3	3.1	<0.0004	<0.0004	<0.0002	<3	0.006	<0.001
Blank - c	05/05/2016	3.2	<22	<137	0.08	0.005	0.18	0.04	0.21	0.01	0.015	2.9	4.2	<0.0004	<0.0004	<0.0002	<3	0.006	<0.001
Blank - f	05/05/2016	4.8	<22	<137	0.14	<0.001	0.09	0.05	0.15	0.01	0.025	3	0.5	0.001	<0.0004	<0.0002	<3	0.005	<0.001

Table 6–1. Trace metal concentrations for sorbent experiment samples and source waters.—Continued

[All trace metal analysis performed at the U.S. Geological Survey Trace Metals Research Laboratory in Boulder, CO. **Abbreviations**: OR, sample was above instrument calibration limit; µg/L, micrograms per liter; <, less than. Letters assigned to each sample represent the total amount of water passed through the filter: 500 mL (A), 1,500 mL (C), and 3,000 mL (F), blank samples were selected at random to be tested and noted with lowercase letters.]

Sample ID	Collection date (mm/dd/yyyy)	Ho	K	La	Li	Lu	Mg	Mn	Mo	Na	Nd	Ni	P	Pb	Pr	Rb	S	Sb	Se	SiO_2
Untreated Source Water (µg/L)																				
Turkey Creek	05/04/2016	0.010	47	0.042	OR	0.004	514	42	1	1,393	0.071	2.8	157	0.36	0.014	102	236	0.13	<2	59
Turkey Creek	05/05/2016	0.008	43	0.076	OR	0.004	483	27	0.4	1,370	0.084	2.8	156	1.4	0.019	94	229	0.12	<2	56
Connate Spring	05/04/2016	0.004	15	0.029	OR	0.002	373	4.2	3.8	749	0.035	13	91	0.51	0.008	2.8	298	0.87	<2	19
Connate Spring	05/05/2016	0.004	14	0.015	OR	0.001	378	1.2	3.5	718	0.02	9.1	98	0.08	0.004	2.6	292	0.83	<2	19
Chitosan (µg/L)																				
Turkey Creek-A	05/04/2016	0.007	47	0.036	OR	0.004	522	13	0.3	OR	0.06	2.2	164	0.27	0.012	105	279	0.097	<2	62
Turkey Creek-C	05/04/2016	0.009	47	0.032	OR	0.004	582	13	0.3	OR	0.065	2.8	180	1.7	0.01	104	288	0.13	<2	66
Turkey Creek-F	05/04/2016	0.009	46	0.029	OR	0.004	523	14	0.4	1,587	0.06	2.4	177	0.68	0.01	100	269	0.11	<2	63
Connate Spring-A	05/04/2016	0.003	16	0.012	OR	0.001	397	1.3	3.9	802	0.013	6.9	98	0.5	0.003	2.8	321	0.92	<2	20
Connate Spring-C	05/04/2016	0.003	16	0.013	OR	0.001	386	0.85	3.7	782	0.014	7.5	84	0.1	0.003	2.7	313	0.89	<2	20
Connate Spring-F	05/04/2016	0.003	15	0.012	OR	0.001	351	0.91	3.8	719	0.015	7.6	79	0.12	0.003	2.7	289	0.87	<2	18
Coconut (µg/L)																				
Turkey Creek-A	05/04/2016	0.011	49	0.044	OR	0.004	548	22	0.8	OR	0.069	2.7	365	0.24	0.013	119	267	0.17	<2	62
Turkey Creek-C	05/04/2016	0.009	47	0.035	OR	0.004	514	18	1	1,422	0.059	2.4	238	0.35	0.012	106	255	0.14	<2	59
Turkey Creek-F	05/04/2016	0.008	46	0.034	OR	0.004	504	16	0.7	1,502	0.059	2.4	207	1.2	0.011	103	248	0.17	<2	58
Connate Spring-A	05/04/2016	0.004	17	0.015	OR	0.002	363	9.2	3.8	727	0.017	8.6	295	0.3	0.004	15	291	0.9	<2	19
Connate Spring-C	05/04/2016	0.003	16	0.017	OR	0.001	382	4.2	3.7	779	0.021	9.6	172	0.47	0.004	6.7	310	0.89	<2	20
Connate Spring-F	05/04/2016	0.003	16	0.015	OR	0.002	394	2.9	3.7	789	0.017	9.0	126	0.16	0.004	4.8	323	0.87	<2	20
Coal (µg/L)																				
Turkey Creek-A	05/05/2016	0.012	44	0.059	OR	0.006	554	33	4.7	1,630	0.087	2.6	176	0.11	0.017	98	271	0.67	<2	63
Turkey Creek-C	05/05/2016	0.012	46	0.043	OR	0.005	577	31	2.4	OR	0.076	2.4	165	0.12	0.014	100	263	0.29	<2	65
Turkey Creek-F	05/05/2016	0.011	46	0.041	OR	0.005	556	32	1.4	OR	0.071	2.4	172	0.12	0.012	103	276	0.2	<2	65
Connate Spring-A	05/05/2016	0.006	15	0.027	OR	0.003	368	2.3	6.1	733	0.032	8.9	83	1.8	0.006	3.9	293	1.2	<2	19
Connate Spring-C	05/05/2016	0.005	16	0.022	OR	0.002	372	1.5	4.9	756	0.024	9.9	91	0.14	0.005	3.4	303	1	<2	19
Connate Spring-F	05/05/2016	0.005	15	0.022	OR	0.002	360	1.2	4	780	0.025	9.8	75	0.38	0.005	3.1	307	0.91	<2	19
Blanks (µg/L)																				
Blank - a	05/05/2016	0.000	0.04	0.003	<0.3	<0.0001	<0.4	0.37	<0.2	<1	0.002	1.50	<12	1.3	0.001	0.014	<0.4	0.018	<2	<0.03
Blank - c	05/05/2016	<0.0001	0.04	0.005	<0.3	<0.0001	<0.4	0.24	<0.2	<1	0.003	0.72	<12	0.48	0.001	0.014	<0.4	0.031	<2	<0.03
Blank - f	05/05/2016	0.000	0.05	0.005	<0.3	<0.0001	<0.4	0.29	<0.2	<1	0.004	0.85	<12	0.13	0.001	0.022	<0.4	0.03	<2	<0.03

Table 6–1. Trace metal concentrations for sorbent experiment samples and source waters.—Continued

[All trace metal analysis performed at the U.S. Geological Survey Trace Metals Research Laboratory in Boulder, CO. **Abbreviations**: OR, sample was above instrument calibration limit; µg/L, micrograms per liter; <, less than. Letters assigned to each sample represent the total amount of water passed through the filter: 500 mL (A), 1,500 mL (C), and 3,000 mL (F), blank samples were selected at random to be tested and noted with lowercase letters.]

Sample ID	Collection date (mm/dd/yyyy)	Sm	Sr	Tb	Te	Th	Ti	Tl	Tm	U	V	Y	Yb	Zn	Zr
Untreated Source Water (µg/L)															
Turkey Creek	05/04/2016	0.023	2,467	0.004	0.09	0.022	<0.5	0.097	0.003	0.067	1.8	0.39	0.021	13	0.044
Turkey Creek	05/05/2016	0.017	2,392	0.004	0.05	0.023	<0.5	0.008	0.003	0.064	1.2	0.36	0.018	69	0.036
Connate Spring	05/04/2016	0.008	1,162	0.002	0.04	0.022	<0.5	0.095	0.002	2.4	4.9	0.19	0.009	49	0.099
Connate Spring	05/05/2016	0.004	1,156	0.002	0.02	0.01	<0.5	0.092	0.001	2.3	4.4	0.17	0.006	43	0.12
Chitosan (µg/L)															
Turkey Creek-A	05/04/2016	0.013	2,625	0.004	0.11	0.021	<0.5	<0.005	0.003	0.081	1.9	0.37	0.022	13	0.039
Turkey Creek-C	05/04/2016	0.017	2,810	0.005	0.09	0.017	<0.5	<0.005	0.003	0.068	1.6	0.39	0.023	23	0.043
Turkey Creek-F	05/04/2016	0.016	2,576	0.005	0.08	0.009	<0.5	0.012	0.003	0.056	1.3	0.38	0.02	16	0.044
Connate Spring-A	05/04/2016	0.004	1,240	0.002	0.04	0.022	<0.5	0.097	0.002	2.6	4.7	0.17	0.008	22	0.14
Connate Spring-C	05/04/2016	0.004	1,213	0.001	0.04	0.02	<0.5	0.097	0.001	2.5	5.2	0.17	0.008	20	0.12
Connate Spring-F	05/04/2016	0.005	1,141	0.002	0.04	0.02	<0.5	0.091	0.001	2.4	5	0.17	0.008	22	0.12
Coconut (µg/L)															
Turkey Creek-A	05/04/2016	0.016	2,583	0.004	0.12	0.016	<0.5	0.023	0.004	0.07	1.4	0.39	0.024	14	0.06
Turkey Creek-C	05/04/2016	0.018	2,500	0.005	0.07	0.015	<0.5	0.019	0.003	0.053	1.6	0.38	0.021	14	0.049
Turkey Creek-F	05/04/2016	0.018	2,422	0.005	0.08	0.025	<0.5	0.01	0.004	0.057	1.7	0.37	0.02	35	0.044
Connate Spring-A	05/04/2016	0.005	1,127	0.001	0.03	0.015	<0.5	0.036	0.001	2.5	4.9	0.16	0.007	35	0.12
Connate Spring-C	05/04/2016	0.005	1,202	0.002	0.03	0.013	<0.5	0.051	0.001	2.6	5.6	0.17	0.008	40	0.11
Connate Spring-F	05/04/2016	0.006	1,255	0.002	0.03	0.014	<0.5	0.06	0.001	2.5	5.2	0.17	0.008	38	0.11
Coal (µg/L)															
Turkey Creek-A	05/05/2016	0.025	2,696	0.007	0.08	0.019	<0.5	0.008	0.006	0.29	1.7	0.65	0.033	14	0.06
Turkey Creek-C	05/05/2016	0.02	2,737	0.006	0.07	0.02	<0.5	0.01	0.005	0.18	1.6	0.54	0.027	13	0.05
Turkey Creek-F	05/05/2016	0.019	2,761	0.006	0.09	0.015	<0.5	0.006	0.004	0.14	1.5	0.5	0.026	15	0.058
Connate Spring-A	05/05/2016	0.009	1,156	0.003	0.03	0.016	<0.5	0.054	0.003	2.5	5.3	0.3	0.012	41	0.12
Connate Spring-C	05/05/2016	0.006	1,192	0.002	0.03	0.011	<0.5	0.065	0.002	2.5	5.2	0.25	0.012	42	0.11
Connate Spring-F	05/05/2016	0.004	1,189	0.002	0.03	0.013	<0.5	0.071	0.002	2.5	5.3	0.23	0.011	42	0.11
Blanks (µg/L)															
Blank - a	05/05/2016	<0.0004	<1.0	<0.0002	<0.02	<0.003	<0.5	<0.005	0.000	<0.009	<0.7	<0.001	<0.0002	2.3	<0.005
Blank - c	05/05/2016	0.000	<1.0	<0.0002	<0.02	<0.003	<0.5	<0.005	0.000	<0.009	<0.7	0.001	0.000	5.9	<0.005
Blank - f	05/05/2016	0.001	<1.0	<0.0002	<0.02	<0.003	0.70	<0.005	<0.00009	0.01	<0.7	0.002	<0.0002	7.6	<0.005

Publishing support provided by the U.S. Geological Survey
Science Publishing Network, Sacramento Publishing Service Center

For more information concerning the research in this report, contact the
Director, California Water Science Center
U.S. Geological Survey
6000 J Street, Placer Hall
Sacramento, California 95819
https://ca.water.usgs.gov

ISSN 2331-1258 (online)
https://doi.org/10.3133/ofr20191001